Article

Cell Reports

AMPK Promotes Xenophagy through Priming of Autophagic Kinases upon Detection of Bacterial Outer Membrane Vesicles

Graphical Abstract

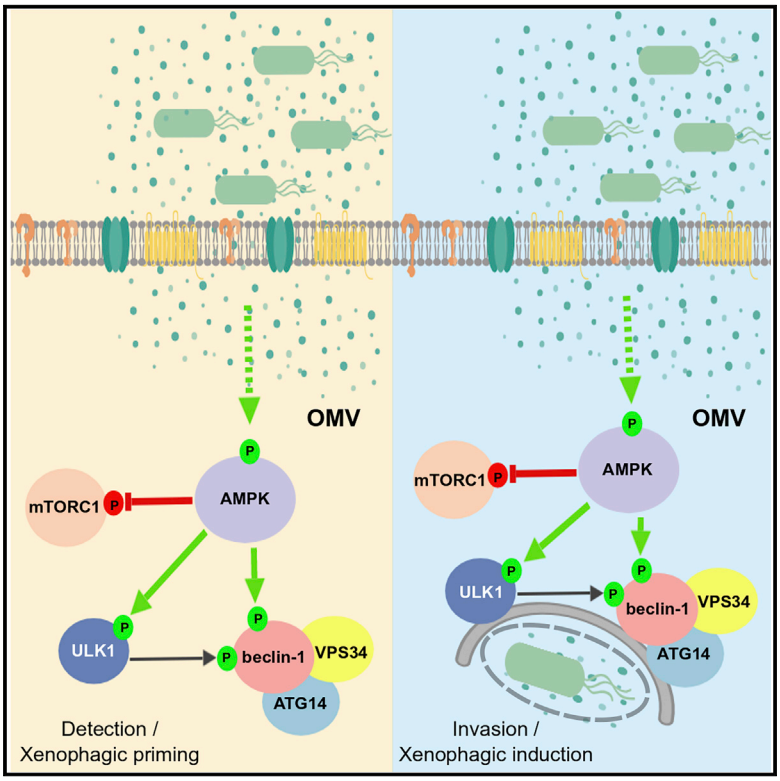

Authors

Truc T. Losier, Mercy Akuma, Olivia C. McKee-Muir, ..., Derrick J. Gibbings, Morgan D. Fullerton, Ryan C. Russell

Correspondence

ryan.russell@uottawa.ca

In Brief

Autophagy is a degradative process that host cells use to cope with invading pathogens, but its earliest activation is unclear. Losier et al. describe a signaling pathway that is activated by the detection of extracellular bacteria-derived OMVs. This autophagy-initiating pathway results in selective targeting and degradation of bacteria rather than cytoplasmic components.

Highlights

- AMPK signaling to the autophagy pathway precedes bacterial invasion
- Bacterial-derived outer membrane vesicles trigger AMPK activation
- Pathogen-induced changes to AMPK and mTORC1 signaling does not induce bulk autophagy
- AMPK is a key regulator of xenophagy through control of mTORC1, ULK1, and VPS34 kinases

Losier et al., 2019, Cell Reports *26*, 2150–2165
February 19, 2019
https://doi.org/10.1016/j.celrep.2019.01.062

CellPress

OPEN ACCESS
CellPress

Cell Reports
Article

AMPK Promotes Xenophagy through Priming of Autophagic Kinases upon Detection of Bacterial Outer Membrane Vesicles

Truc T. Losier,[1,3] Mercy Akuma,[1,3,5] Olivia C. McKee-Muir,[1,3,5] Nicholas D. LeBlond,[2,3] Yujin Suk,[1,3] Reham M. Alsaadi,[1,3] Zhihao Guo,[1,3] Ryan Reshke,[1,3] Subash Sad,[2,3] François-Xavier Campbell-Valois,[2,4] Derrick J. Gibbings,[1,3] Morgan D. Fullerton,[2,3] and Ryan C. Russell[1,3,6,*]

[1]Department of Cellular and Molecular Medicine, University of Ottawa, 451 Smyth Road, Ottawa, ON K1H 8M5, Canada
[2]Department of Biochemistry, Microbiology and Immunology, University of Ottawa, 451 Smyth Road, Ottawa, ON K1H 8M5, Canada
[3]University of Ottawa Center for Infection, Immunity, and Inflammation, Ottawa, ON K1H 8M5, Canada
[4]Department of Chemistry and Biomolecular Sciences, University of Ottawa, Pavillon D'Iorio Hall, 10 Marie Curie, Ottawa, ON K1N 6N5, Canada
[5]These authors contributed equally
[6]Lead Contact
*Correspondence: ryan.russell@uottawa.ca
https://doi.org/10.1016/j.celrep.2019.01.062

SUMMARY

The autophagy pathway is an essential facet of the innate immune response, capable of rapidly targeting intracellular bacteria. However, the initial signaling regulating autophagy induction in response to pathogens remains largely unclear. Here, we report that AMPK, an upstream activator of the autophagy pathway, is stimulated upon detection of pathogenic bacteria, before bacterial invasion. Bacterial recognition occurs through the detection of outer membrane vesicles. We found that AMPK signaling relieves mTORC1-mediated repression of the autophagy pathway in response to infection, positioning the cell for a rapid induction of autophagy. Moreover, activation of AMPK and inhibition of mTORC1 in response to bacteria is not accompanied by an induction of bulk autophagy. However, AMPK signaling is required for the selective targeting of bacteria-containing vesicles by the autophagy pathway through the activation of pro-autophagic kinase complexes. These results demonstrate a key role for AMPK signaling in coordinating the rapid autophagic response to bacteria.

INTRODUCTION

Macroautophagy (hereafter referred to as autophagy) is a heavily regulated degradative process activated by a range of cellular stressors, including nutrient starvation, proteotoxic aggregates, and pathogen infection (Kaur and Debnath, 2015). Autophagy is driven by a set of highly conserved "autophagy related" (ATG) proteins, which stimulate the *de novo* formation of a double-membrane vesicle called an autophagosome (Kaur and Debnath, 2015). The fully formed autophagosome achieves its degradative potential after fusion with the lysosome, which provides the acid hydrolases responsible for the breakdown of sequestered macromolecules (Mizushima and Klionsky, 2007).

Autophagy initiation is tightly regulated by the activity of the protein kinase ULK1 (Unc-51-like kinase-1) and the lipid kinase VPS34. Recruitment of ULK1 to the site of autophagosome formation (in mammals, this is called the phagophore) is one of the first detectable events in autophagy initiation (Itakura and Mizushima, 2010). ULK1 activity is tightly regulated through inhibitory phosphorylation by the mTORC1 (mechanistic target of rapamycin complex 1) kinase (Jung et al., 2009; Hosokawa et al., 2009; Ganley et al., 2009) and activating phosphorylation by AMPK (AMP-activated kinase) (Kim et al., 2011). Different cellular stressors, including nutrient starvation, ROS (reactive oxygen species) accumulation, and reduced cytokine signaling, are capable of activating autophagy by shifting the balance of activating and inhibitory phosphorylation of ULK1 by mTORC1 and AMPK (Russell et al., 2014). Once activated, ULK1 phosphorylates a transmembrane protein called ATG9 and multiple subunits of the pro-autophagic VPS34 complexes (Nazio et al., 2013; Russell et al., 2013; Park et al., 2016). ULK1-mediated recruitment of VPS34 to the phagophore is required for autophagy initiation. At the phagophore, VPS34 phosphorylates phosphatidylinositol (PtdIns) to produce PtdIns(3)phosphate (PtdIns(3)P). PtdIns(3)P production is responsible for the recruitment of downstream components of the autophagy pathway and is indispensable for autophagosome formation. In addition, AMPK and mTORC1 have been described as directly regulating the activity of the VPS34 kinases, thus ensuring a tightly controlled burst of autophagy initiation in response to cellular stresses and underscoring the importance of VPS34 regulation (Yuan et al., 2013; Kim et al., 2013).

Autophagy plays an important role in sequestering intracellular bacteria and delivering them to the lysosome for neutralization (Gomes and Dikic, 2014). As such, vacuolar bacteria, including *Salmonella enterica* serovar Typhimurium (hereafter referred to as *Salmonella*), have evolved approaches to inhibit their delivery to the lysosomal compartment (Huang and Brumell, 2014). Avoidance of autophagy by *Salmonella* has been described best through the actions of bacterial effector proteins injected

into the host cytosol by the type III secretion system (T3SS), which aids in the avoidance of the autophagy pathway and remodeling of the *Salmonella*-containing vacuole (SCV) to promote *Salmonella* growth. However, it has recently been found that the membrane damage caused by the T3SS can be recognized by the host and result in autophagic clearance of the SCV (Boyle and Randow, 2013). As a result, *Salmonella* replication is higher in autophagy-deficient cells (Huett et al., 2012). *Salmonella* can also be targeted to the lysosomal compartment through a process called LC3-associated phagocytosis (LAP) (Sanjuan et al., 2007; Huang et al., 2009). LAP is a biologically and mechanistically distinct pathway from autophagy and is independent of core autophagy proteins, including ULK1 and autophagy adaptors such as sequesterosome 1 (p62), which bind ubiquitin and LC3B (Martinez et al., 2015; Sanjuan et al., 2007; Martinez et al., 2011).

Anti-bacterial autophagy (hereafter referred to as xenophagy) requires the core autophagy machinery as well as specialized mechanisms for targeting vacuolar *Salmonella*. For example, damaged SCVs are cleared through the action of galectin 8 (Thurston et al., 2012) and autophagy adaptors, including nuclear domain 10 protein 52 (NDP52) (Li et al., 2013), optineurin (OPTN) (Wild et al., 2011), and p62 (Zheng et al., 2009). Recent work on xenophagy regulation has uncovered a significant overlap between signaling in starvation- and pathogen-induced autophagy. For example, membrane damage from *Salmonella* has been described as inducing a transient reduction in intracellular amino acid levels, which alleviates mTORC1-mediated repression of the autophagy pathway (Tattoli et al., 2012b). In addition, immunity-related guanosine triphosphatase (GTPase) M (IRGM) has been shown to bind and/or regulate several factors involved in autophagy initiation, including the VPS34 kinase complex, ULK1, and AMPK (Chauhan et al., 2015). The loss of IRGM does not abrogate starvation-induced autophagy, but it is required for the efficient clearance of bacteria and is the most commonly targeted component of the autophagy pathway by RNA viruses (Grégoire et al., 2011). These studies highlight the fact that the induction of xenophagy involves several of the same upstream signaling regulators used in starvation-induced autophagy, which are coupled with bacterial stress-specific factors to coordinate the cellular response to pathogens. However, the precise signaling upstream of the autophagy pathway in response to bacterial infection and the specificity of these signals remain to be elucidated. Here, we describe a signaling event that "primes" the cell to induce xenophagy independently of bacterial entry. We also show that unlike nutrient starvation, pathogen-induced regulation of mTORC1 and AMPK does not result in an increase in bulk autophagy. Finally, we characterize AMPK signaling to the autophagy pathway in response to *Salmonella* infection and its physiological role in xenophagy induction.

RESULTS

AMPK Is Activated by *Salmonella* and Directly Inhibits mTORC1

AMPK and mTORC1 signaling are critical upstream regulators in starvation-induced autophagy (Kim et al., 2011; Yuan et al., 2013; Ganley et al., 2009; Hosokawa et al., 2009; Jung et al., 2009; Egan et al., 2011). Previous reports have described that *Salmonella* infection can result in either mTORC1 activation or inhibition (Tattoli et al., 2012b; Ganesan et al., 2017). To determine the key upstream signaling events regulating xenophagy induction, we infected colon epithelial cells (HCT116) and bone marrow-derived macrophages (BMDM) with *Salmonella* and determined the phosphorylation status of established AMPK-target acetyl-coenzyme A (CoA) carboxylase (ACC) and mTORC1-target ribosomal protein S6 kinase (S6K), which migrates as doublets in some cell lines. Consistent with previous reports, we found that mTORC1 activity is inhibited in colon epithelial cells, but activated in macrophages (Figure 1A) (Ganesan et al., 2017; Tattoli et al., 2012b). However, we found that AMPK is activated in both colon epithelial cells and macrophages upon *Salmonella* infection by measuring changes in the AMPK-mediated phosphorylation of ACC (Figure 1A). Since both epithelial cells and macrophages are capable of inducing xenophagy, this raises the possibility that AMPK activation may be the primary signaling pathway responsible for the activation of the autophagy kinases in the response to infection.

We next sought to expand the analysis of AMPK regulation by *Salmonella* infection in multiple cell lineages, including kidney (HEK293A), lung (A549), fibroblast (mouse embryonic fibroblast [MEF]), and breast epithelia (MCF-7). We observed a potent activation of AMPK and repression of mTORC1 signaling as measured by downstream target phosphorylation in all of the cell lines tested (Figure 1B). These results suggest that aside from in macrophages, AMPK activation and mTORC1 inhibition are the conserved responses to *Salmonella* infection. We found that other Gram-negative bacteria, including *Shigella flexneri and* adherent invasive *Escherichia coli* (AIEC) also elicited a potent activation of AMPK (Figure S1A). As the xenophagic response is better defined in *Salmonella* than in *Shigella* or AIEC, we continued our characterization of xenophagy regulation using *Salmonella* as our model pathogen. We next confirmed that the regulation of AMPK and mTORC1 signaling by *Salmonella* was consistent across various MOIs reported in the literature. We found consistent effects on signaling from an MOI of 10–450, with a delay in signaling at a lower MOI (Figure S1B). However, the amplitude signaling changes at each MOI were consistent at peak induction (Figure S1C). We moved forward with an MOI of 450, which in HCT116 cells at 1 h gives an infection rate of 10% (Figure S1D).

A previous report in macrophages suggested that Sirt-1 stability is an important regulator of mTORC1 activity, having a maximal effect at 4–5 h post-infection, which is considerably later than the 1-h time point we selected (Ganesan et al., 2017). To determine whether Sirt-1 stability plays a role in non-macrophages at a later time point, we performed a temporal analysis of AMPK and mTORC1 signaling in response to *Salmonella* infection. We found that the activation of AMPK and the inhibition of mTORC1 begin at 1 h post-infection and occur in the absence of changes to Sirt-1 levels at all of the time points tested (Figure 1C). These results indicate that the regulation of mTORC1 in epithelial cells does not require the destabilization of Sirt-1.

Membrane damage caused by *Salmonella* infection has been shown to result in amino acid loss and mTORC1 inhibition (Tattoli

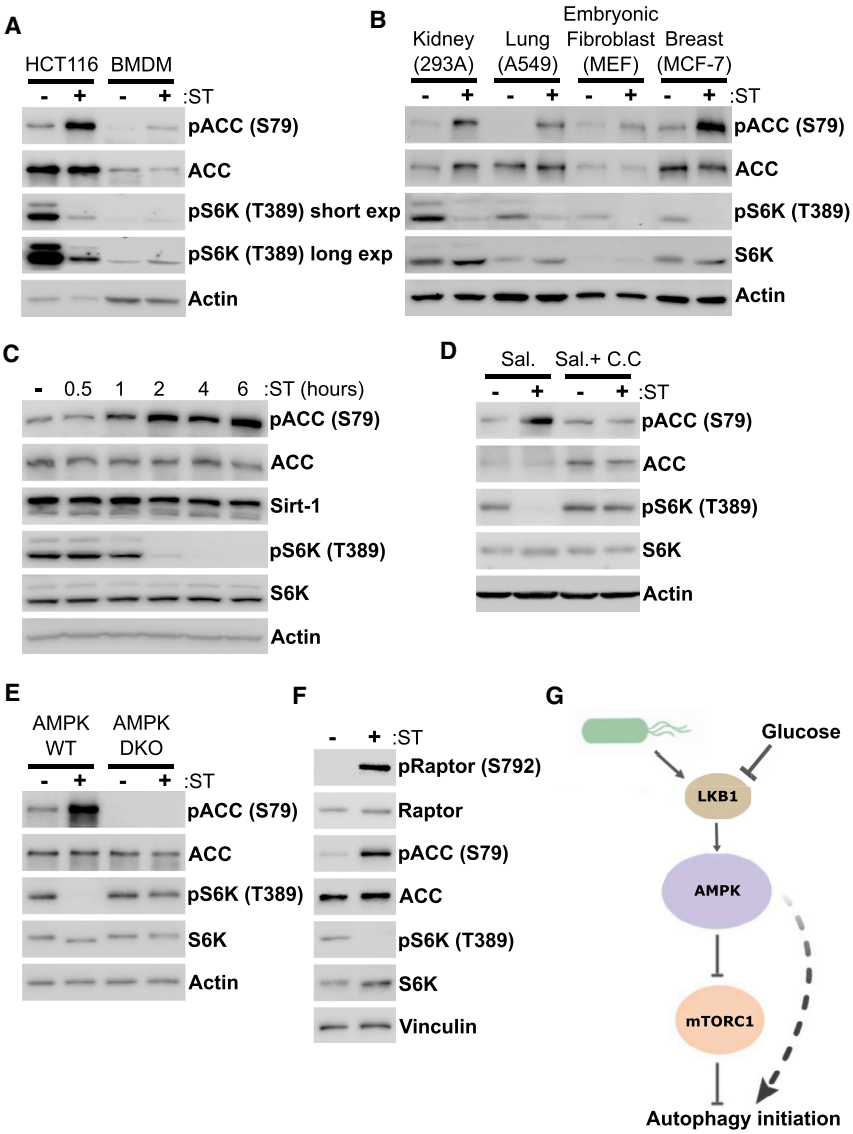

Figure 1. *Salmonella enterica* Serovar Typhimurium Regulates AMPK and mTORC1 Activity

(A) HCT116 cells and bone marrow-derived macrophages (BMDMs) were infected with log phase *Salmonella* (ST) (unless otherwise stated, an MOI of 450 was used) for 1 h. Samples were immunoblotted for targets of mTORC1 (phospho-S6K) and AMPK (phospho-ACC).

(B) HEK293A, A549, MEF, and MCF-7 cells were treated with *Salmonella* for 1–1.3 h. Whole-cell lysates were immunoblotted using the antibodies indicated.

(C) HCT116 cells were treated with *Salmonella* and lysed at the indicated time points. Samples were immunoblotted using the antibodies indicated.

(D) AMPK was activated by salicylate (Sal.) and HCT116 cells were infected with *Salmonella* in the presence or absence of AMPK inhibitor compound C (C.C.). Whole-cell lysates were immunoblotted using the antibodies indicated.

(E) AMPK wild-type (WT) and deficient (AMPK α1/2 knockout) MEF cells were infected with *Salmonella* for 1.3 h. mTORC1 and AMPK activities were analyzed using the indicated antibodies.

(F) HEK293A cells were infected with *Salmonella* for 1.3 h. AMPK-mediated inhibition of the mTORC1 subunit Raptor (phosphorylation of Raptor at S792) was analyzed by western blot.

(G) Diagram of signaling (A)–(F).

Unless otherwise indicated, experiments were performed three times.

See also Figure S1.

et al., 2012b). However, AMPK is also known to inhibit mTORC1 directly and indirectly in an amino acid-independent manner (Gwinn et al., 2008). This led us to ask whether AMPK signaling contributes to mTORC1 inhibition upon infection. To monitor the effects of AMPK signaling on mTORC1, we infected cells in the absence or presence of compound C, which is a potent inhibitor of AMPK most often used in conjunction with AMPK activators such as salicylate (Zhou et al., 2001; Hawley et al., 2012). We found that *Salmonella*-induced inhibition of mTORC1 is blocked by AMPK inhibitors, indicating that AMPK signaling contributes to the inhibition of mTORC1 independently of regulation by amino acids (Figure 1D). To confirm that AMPK signaling is responsible for the reduction in mTORC1 signaling, we infected the AMPK α1 and α2 (the catalytic subunits of AMPK) double knockout MEFs and analyzed mTORC1 activity. We found that *Salmonella*-induced inhibition of mTORC1 signaling is greatly reduced in the AMPK double knockout MEFs, indicating that AMPK signaling promotes the inhibition of mTORC1 upon infection independent of amino acid loss (Figure 1E).

AMPK can inhibit mTORC1 through multiple mechanisms. Arguably, the most potent and direct mechanism is AMPK-mediated inhibitory phosphorylation of the mTORC1 subunit Raptor (Shaw et al., 2004; Gwinn et al., 2008). Therefore, we sought to determine whether *Salmonella* infection results in an increase in direct inhibition of the mTORC1 kinase by AMPK. Cells were infected with *Salmonella*, and inhibitory phosphorylation of the mTORC1 subunit Raptor by AMPK was analyzed in conjunction with AMPK and mTORC1 target genes. We found that *Salmonella* infection results in a potent upregulation of Raptor phosphorylation and mTORC1 inhibition (Figure 1F). Finally, we determined that liver kinase B-1 (LKB1), an upstream activator of AMPK, is required for the activation of AMPK and the inhibition of mTORC1 in response to *Salmonella* (Figure S1E). These experiments establish that in response to *Salmonella*, mammalian cells activate AMPK (an upstream activator of the autophagy pathway), which in turn directly inhibits mTORC1 (a potent repressor of autophagy initiation), thereby setting the stage for autophagy initiation (Figure 1G).

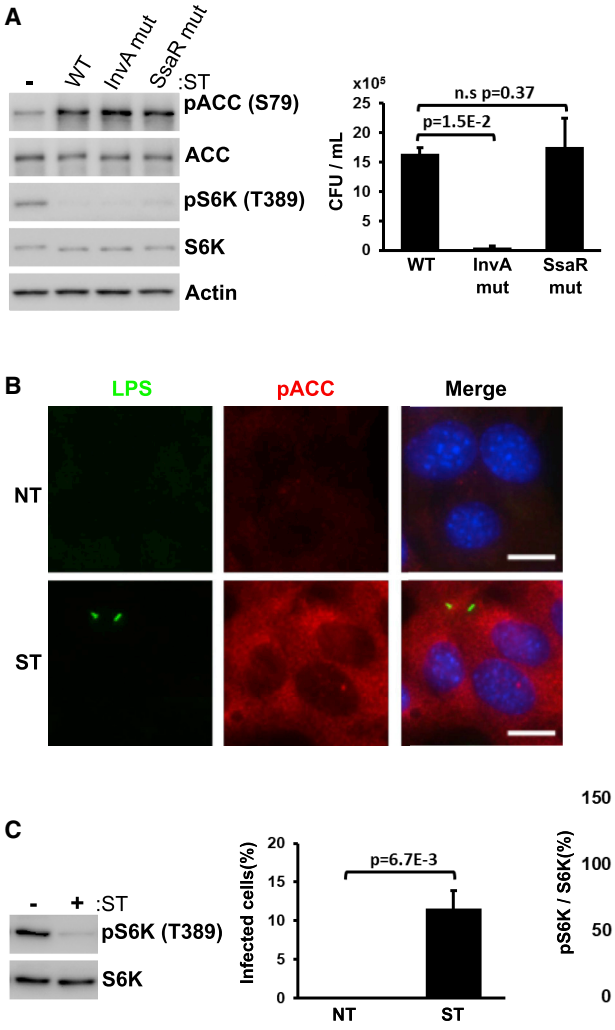

Figure 2. AMPK Activity Is Independent of *Salmonella* Pathogenicity and Invasion

(A) HCT116 cells were infected with wild-type, invasion-deficient (InvA mutant), or replication-deficient (SsaR mutant) *Salmonella* (unless otherwise stated, an MOI of 450 was used) for 1 h. Xenophagy rates were examined through colony-forming unit (CFU) assays. Whole-cell lysates were immunoblotted for AMPK and mTORC1 activities using the antibodies indicated.

(B) MEF cells were infected with *Salmonella* for 1 h. Immunostaining was performed for AMPK-mediated phosphorylation of ACCs and LPSs. Scale bars, 16 μM.

(C) Inhibition of mTORC1 was quantified from western blot data derived from biological replicates and compared to the overall infection rate to examine whether mTORC1 inhibition could be explained by the proportion of cells with bacterial internalization.

Unless otherwise indicated, experiments were performed three times. Data are represented as means ± SDs, and p values were determined by Student's t test.

See also Figure S2.

Salmonella-Induced Changes to AMPK-mTORC1 Signaling Do Not Require Bacterial Entry or SCV Damage

Changes in mTORC1 signaling and the resulting activation of xenophagy have been described exclusively in the context of internalized bacteria (Tattoli et al., 2012a, 2012b; Owen et al., 2014; Ganesan et al., 2017). Inhibition of mTORC1 upon infection has been shown to promote the clearance of intracellular bacteria by xenophagy (Owen et al., 2014). Similarly, AMPK activation has been proposed to be a result of membrane damage caused by bacterial internalization, which leads to a loss in intracellular ATP levels, thereby activating AMPK (Ganesan et al., 2017). Intracellular expansion of *Salmonella* is promoted by two T3SSs, encoded by two pathogenicity islands (SPI-1 and SPI-2), which promote invasion and intracellular survival, respectively (Galán and Curtiss, 1989; Ochman et al., 1996; Hensel et al., 1995). Membrane damage caused by *Salmonella* occurs during invasion (SPI-1 dependent) as well as through the disruption of the SCV (SPI-2 dependent) (Tattoli et al., 2012a).

To determine whether membrane damage is responsible for the activation of AMPK, we infected cells with wild-type *Salmonella*, invasion-deficient SPI-1 mutants (InvA null) (Galán and Curtiss, 1991), or replication-compromised SPI-2 mutants (SsaR null) (Cirillo et al., 1998) and assayed for AMPK activation and mTORC1 inhibition. Colony-forming assays were performed from cell lysates 1 h post-infection to confirm the invasion deficiency of SPI-1 mutants (Figure 2A, right). We found that AMPK activation was still observed in *Salmonella* that was defective for invasion and SCV disruption (Figures 2A and S2A). Similarly, mTORC1 inhibition is also observed upon infection with all three *Salmonella* strains (Figure 2A). This indicates that AMPK activation likely does not require membrane damage that is associated with bacterial entry or disruption of the SCV. To analyze AMPK activation by *Salmonella* at a single-cell level, we infected cells immunostained for AMPK-mediated phosphorylation of ACC and *Salmonella*. Using identical acquisition settings, we saw a clear increase in AMPK-target phosphorylation upon treatment with *Salmonella* (Figure 2B). In *Salmonella*-treated cells, we observed AMPK activation homogenously throughout the sample, with no difference between cells with or without internalized bacteria (Figure 2B, bottom right). These data further support the notion that AMPK activation is due to extracellular bacteria independent of invasion or pathogenicity. Next, we sought to determine whether removing extracellular *Salmonella* is sufficient to return AMPK and mTORC1 signaling to basal levels. Extracellular bacteria were removed in one set of samples or left on in another, before lysis. However, cells were infected and treated with gentamycin for the same duration, which controlled for the potential effects of the antibiotic on signaling and produced an equivalent rate of

infection (Figure S2B). Consistent with previous data, we observed that the removal of extracellular *Salmonella* resulted in a loss of AMPK activity and the restoration of mTORC1 signaling (Figure S2B).

Finally, we sought to show mathematically the independence of AMPK-mTORC1 signaling and bacterial entry through the analysis of infection rates and mTORC1 inhibition. As in the previous sets of experiments, we analyzed samples by western blotting and immunofluorescence (IF) using duplicated sample preparation. However, to obtain the highest possible estimate for the percentage of infected cells, we infected the cells in the presence of an inhibitor of autophagic flux, bafilomycin A1, thereby blocking autophagic clearance of bacteria, which could cause an underrepresentation of the actual number of infected cells. Using these stringent conditions, we found that approximately 10% of cells contain internalized bacteria and that mTORC1 activity is inhibited >90% (Figure 2C). Under these conditions, we would expect that if internalized bacteria were required for mTORC1 inhibition, then the inhibition should only approach 10% (the proportion of cells infected) rather than the 90% we observed. Finally, we determined that AMPK activation could be elicited by the filtered supernatant from pelleted *Salmonella,* indicating that bacterial internalization is not essential for the activation of AMPK in mammalian cells (Figure S2C).

Our data show that the regulation of AMPK and mTORC1 signaling can occur independently of *Salmonella* pathogenicity and invasion. Conceptually, this is extremely interesting, as it means that the cell is poised to activate xenophagy even before the bacteria enter the cell.

Salmonella-Induced Signaling to AMPK and mTORC1 Does Not Result in an Induction of Bulk Autophagy

mTORC1 is a potent repressor of mammalian autophagy and directly inhibits the ULK1 and VPS34 kinase complexes, which are required for autophagy initiation (Jung et al., 2009; Hosokawa et al., 2009; Ganley et al., 2009; Yuan et al., 2013). The removal of amino acids is sufficient to dissociate mTORC1 from the lysosome and potently activate autophagy. We therefore sought to observe whether mTORC1 localization and autophagy induction are similarly affected by host cell detection of *Salmonella*. We treated cells either with *Salmonella* or amino acid withdrawal. As expected, the localization of mTORC1 was primarily lysosomal under basal conditions as determined by co-localization between mTOR and lysosomal marker lysosomal-associated membrane protein 1 (LAMP1) (Figure 3A). We found that both amino acid starvation and extracellular *Salmonella* greatly reduce the localization of mTOR to the lysosome (Figure 3A). The observed loss of mTORC1 localization from lysosomes under starvation or infection should both result in a de-repression of autophagy initiation.

We next sought to determine whether inhibition of mTORC1 by *Salmonella* increases autophagy in uninfected cells. As expected, amino acid withdrawal results in a potent increase in autophagosome formation in the majority of cells as determined quantification of immunostaining for endogenous LC3B puncta (Figure 3B). We were surprised that we did not observe a similar induction in bulk autophagy in *Salmonella*-treated cells (Figure 3B). Moreover, while we observed endogenous LC3B colocalization to internalized bacteria, we found that infected cells similarly did not display an increase in bulk autophagy (Figures 3B and S3A). These data indicate that mTORC1 inhibition in response to *Salmonella* is not sufficient to induce autophagy, and the autophagic activity we observed is largely limited to the targeting of pathogens, sparing cytoplasmic constituents. To further verify the regulation of autophagy in response to *Salmonella*, we analyzed the autophagic adaptor p62, which mark bacteria targeted for clearance by autophagy, as well as starvation-induced autophagosomes, but not bacteria captured by LC3-associated phagocytosis (LAP). Immunostaining for endogenous p62 shows a dramatic induction bulk autophagy upon amino acid starvation (Figure 3C). However, consistent with our LC3B staining, we did not observe any increase in p62-associated bulk autophagy in *Salmonella*-treated cells, even with internalized bacteria (Figures 3C and S3B).

To confirm the effects of infection on the autophagy pathway, we next analyzed autophagy flux under infection and starvation. Cells were treated with *Salmonella* or amino acid withdrawal in the presence or absence of an inhibitor for autophagosomal turnover (chloroquine), and we measured the accumulation of lipidated LC3B by western blot. We observed a robust accumulation of lipidated LC3B upon amino acid starvation but not *Salmonella* treatment when compared to untreated samples (Figure 3D).

We next sought to compare the levels of AMPK activation and mTORC1 inhibition by established methods to induce bulk autophagy to the signaling changes induced by *Salmonella*. We observed that AMPK activation by glucose starvation was higher but comparable to that induced by infection (Figure 3E). Similarly, mTORC1 signaling was undetectable after Torin-1 treatment, but still comparable to the inhibition elicited by *Salmonella* (Figure 3E). However, analysis of the clearance of the autophagy adaptor p62 clearly showed that the induction of bulk autophagy by glucose starvation or Torin-1 treatment was absent in the cells infected with either wild-type or invasion-deficient *Salmonella*. This indicates that a blockage of autophagy induction may be present downstream of mTORC1 and AMPK upon *Salmonella* infection.

ULK1 kinase is a direct downstream target of both AMPK and mTORC1. Under starvation, ULK1 is activated and localizes to newly forming autophagosomes to phosphorylate downstream targets required to promote autophagosome formation. Therefore, we next analyzed the subcellular localization of ULK1 to determine whether autophagy initiation is blocked under infection downstream of mTORC1. As expected, when mTORC1 was inhibited by amino acid starvation, we found a robust increase in punctate ULK1 structures, which is indicative of bulk autophagy (Figure 3F) (Park et al., 2016). However, under infection, we observed a lack of ULK1 puncta, aside from those targeting *Salmonella* (Figure S3C), indicating that the *Salmonella*-induced autophagy block is at ULK1 or upstream of ULK1 (Figure 3F).

To determine whether *Salmonella* was eliciting a blockage of autophagy induction downstream of mTORC1, we treated cells with wild-type or InvA mutant *Salmonella* in the presence or absence of Torin-1. We observed that both wild-type and InvA null bacteria eliminate Torin-1-induced bulk autophagy, as

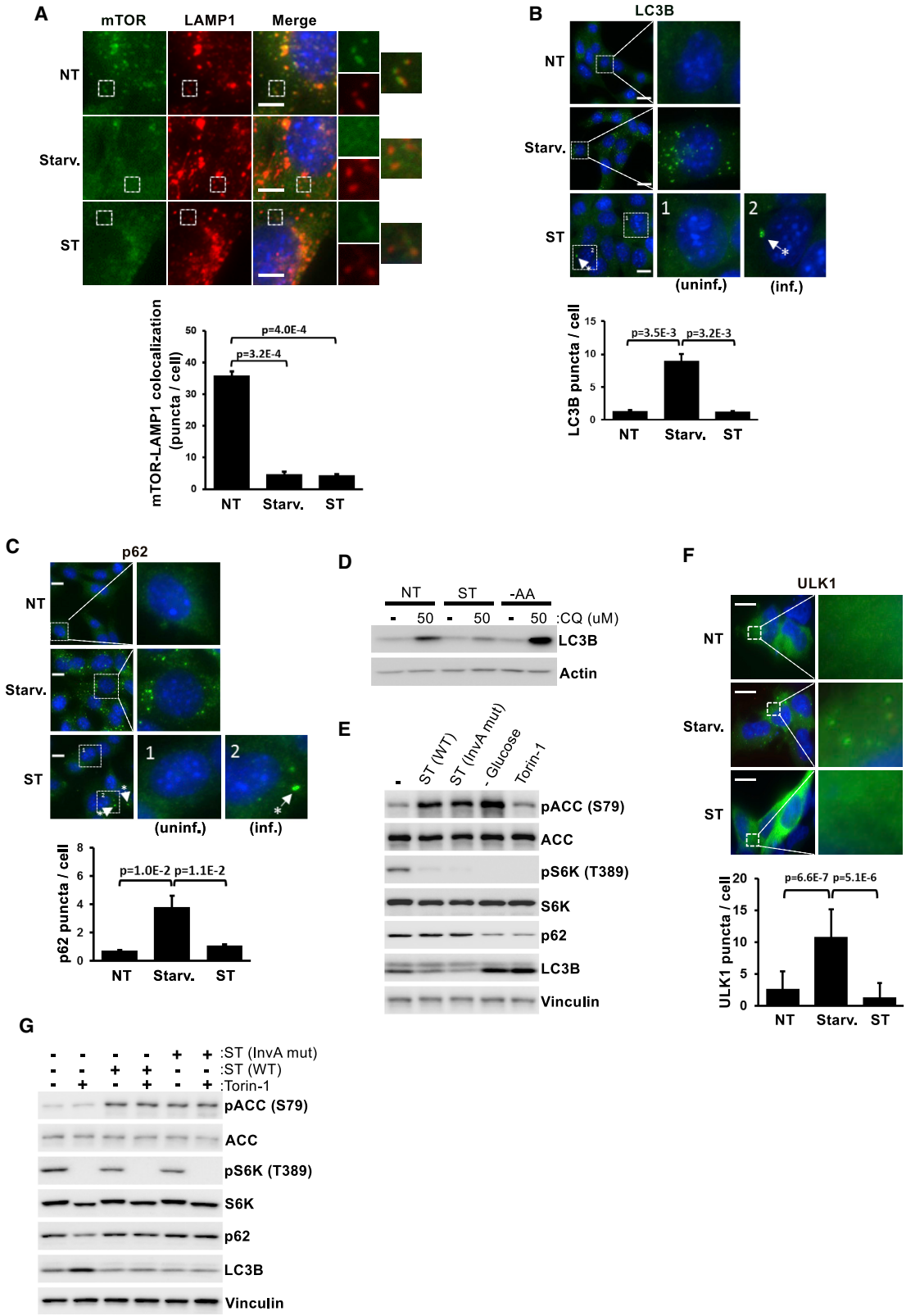

(legend on next page)

measured by LC3B lipidation and p62 clearance, confirming an inhibitory pathway decoupling mTORC1 inhibition from autophagy induction (Figures 3G and S3D). These data reveal a surprising level of specificity in the regulation of xenophagy induction. This raises the exciting possibility that in response to *Salmonella* detection, the cell initiates signaling events that prime the cell for autophagic clearance of the bacteria without needlessly degrading components of the cytosol through the induction of bulk autophagy.

AMPK Activates ULK1 and VPS34 Kinases in Response to *Salmonella*

To determine whether regulation of mTORC1 and AMPK signaling is capable of activating autophagy-promoting enzymes in the absence of bulk autophagy induction, we looked at the phosphorylation of the ULK1 protein kinase. ULK1 activity has been described as being inhibited by mTORC1-mediated phosphorylation (Ser757) and activated by AMPK-mediated phosphorylation (Ser317) under nutrient starvation (Kim et al., 2011). Using 293A cells stably expressing tagged ULK1, we immunoprecipitated ULK1 treated with or without *Salmonella* and immunoblotted for activating or inhibitory ULK1 phosphorylation. We observed that despite the lack of bulk autophagy, ULK1 is phosphorylated by AMPK and experiences a reduction in mTORC1-mediated phosphorylation, both of which should lead to the activation of kinase activity (Figure 4A). To ascertain whether ULK1 activity is induced and whether this activity is dependent on AMPK signaling, we transfected tagged ULK1 into AMPK wild-type and α1/2 knockout MEFs and performed an *in vitro* kinase assay using bacterially purified beclin-1, a known downstream target (Russell et al., 2013), as substrate. We observed that the kinase activity of ULK1, measured by beclin-1 (Ser15) phosphorylation, is increased upon infection in wild-type MEFs but not AMPK-deficient cells (Figure 4B), indicating that AMPK signaling promotes ULK1 activation in response to *Salmonella* detection.

In addition to regulating ULK1 activity, AMPK has been shown to promote the activity of proautophagic VPS34 lipid kinase complexes through direct phosphorylation (Kim et al., 2013). Therefore, we next sought to determine whether autophagy-promoting signaling from AMPK extends to VPS34, which is downstream of ULK1 in autophagy initiation. In response to glucose deprivation, AMPK was previously shown to phosphorylate VPS34 component beclin-1 (on Ser93), which is sufficient to increase the activity of VPS34 containing enzymes (Kim et al., 2013). We found that *Salmonella* treatment results in a robust increase in endogenous beclin-1 phosphorylation by AMPK (Figure 4C). Next, we sought to examine the activation of ULK1 and VPS34 kinases in comparison to amino acid and energy starvation. We observed that ULK1 activation, as measured by an increase in AMPK-mediated phosphorylation (S317) and a loss of mTORC1-mediated inhibitory phosphorylation (S757), was similar to that induced by glucose starvation (Figure 4D). We consistently observed a roughly equivalent AMPK-mediated activation of VPS34, indicating that AMPK-driven signaling by energy starvation and *Salmonella* infection were comparable in promoting the activation of autophagy kinases (Figure 4D).

We then sought to determine whether the activity of proautophagic VPS34 complexes (those that contain beclin-1 and autophagy-related 14 [ATG14]) are increased upon treatment with *Salmonella*. The 293A cells transiently transfected with tagged ATG14 were treated with or without *Salmonella*, and ATG14-containing VPS34 complexes were immunoprecipitated and analyzed by an *in vitro* lipid kinase assay and dot-blot assay, as previously described (Park et al., 2016). We found that *Salmonella* treatment results in a significant upregulation of VPS34 activity, as measured by the production of PtdIns(3)P from PtdIns (Figure 4E). Next, we sought to analyze the regulation of VPS34 activity endogenously. MEFs were treated with or without *Salmonella*, and endogenous ATG14-containing VPS34 complexes were immunoprecipitated and subjected to an *in vitro* lipid kinase assay. Consistent with our observation that *Salmonella* infection promotes AMPK-mediated activation of beclin-1-containing VPS34 complexes, we observed that the activity of VPS34 is enhanced upon exposure to *Salmonella* (Figure 4F). Our data indicate that AMPK-mediated phosphorylation of the ULK1 and VPS34 kinase complexes results in their activation in response to *Salmonella* treatment, despite the absence of bulk autophagy induction (Figure 4G). Moreover, we found that similar to *wild-type*, InvA mutant *Salmonella* is also capable of activating ULK1 and VPS34 kinases in both epithelial cells and macrophages (Figures S4A–S4D). This raises the possibility that the detection of pathogens results in an AMPK-dependent "priming" of key autophagy kinases that are responsible for the induction of xenophagy, which may act to enhance the rate of bacterial capture by the autophagy pathway should invasion occur.

Figure 3. *Salmonella*-Mediated AMPK and mTORC1 Regulation Does Not Induce Bulk Autophagy

(A) MEF cells were treated with either full medium, starvation medium (Hank's balanced salt solution [HBSS]), or *Salmonella* for 1 h. LAMP1 (red, lysosomal marker) and mTOR (green) co-localization was visualized and quantified by immunofluorescence. Scale bars, 8 μM.

(B and C) MEF cells were treated with either full medium, starvation medium (HBSS), or *Salmonella* for 1 h. Either LC3B (B) puncta or p62 (C) was visualized and quantified by immunofluorescence. Scale bars, 16 μM.

(D) MEF cells were treated with either full medium, *Salmonella,* or starvation medium and with or without 50 μM chloroquine (CQ) for 1 h. LC3B signaling was then analyzed by western blot.

(E) MEF cells were treated with either *Salmonella* (wild-type), *Salmonella* (InvA mutant), glucose starvation medium, or 0.2 μM Torin-1 (mTORC1 inhibitor) for 1 h. Western blot was used to examine autophagy flux (LC3B lipidation and p62 clearance).

(F) HEK293A cells transiently expressing glutathione S-transferase (GST) hemagglutinin (HA) ULK1 were treated with either full medium, amino acid starvation medium, or *Salmonella* for 1.33 h. The HA tag was immunostained to demonstrate ULK1 localization. Scale bars, 16 μM.

(G) MEF cells were treated with either *Salmonella* (wild-type) or *Salmonella* (InvA mutant) in the presence or absence of Torin-1 for 1 h. Autophagy markers LC3B and p62 were then analyzed by western blot.

Unless otherwise indicated, experiments were performed three times. Data are represented as means ± SDs, and p values were determined by Student's t test. See also Figure S3.

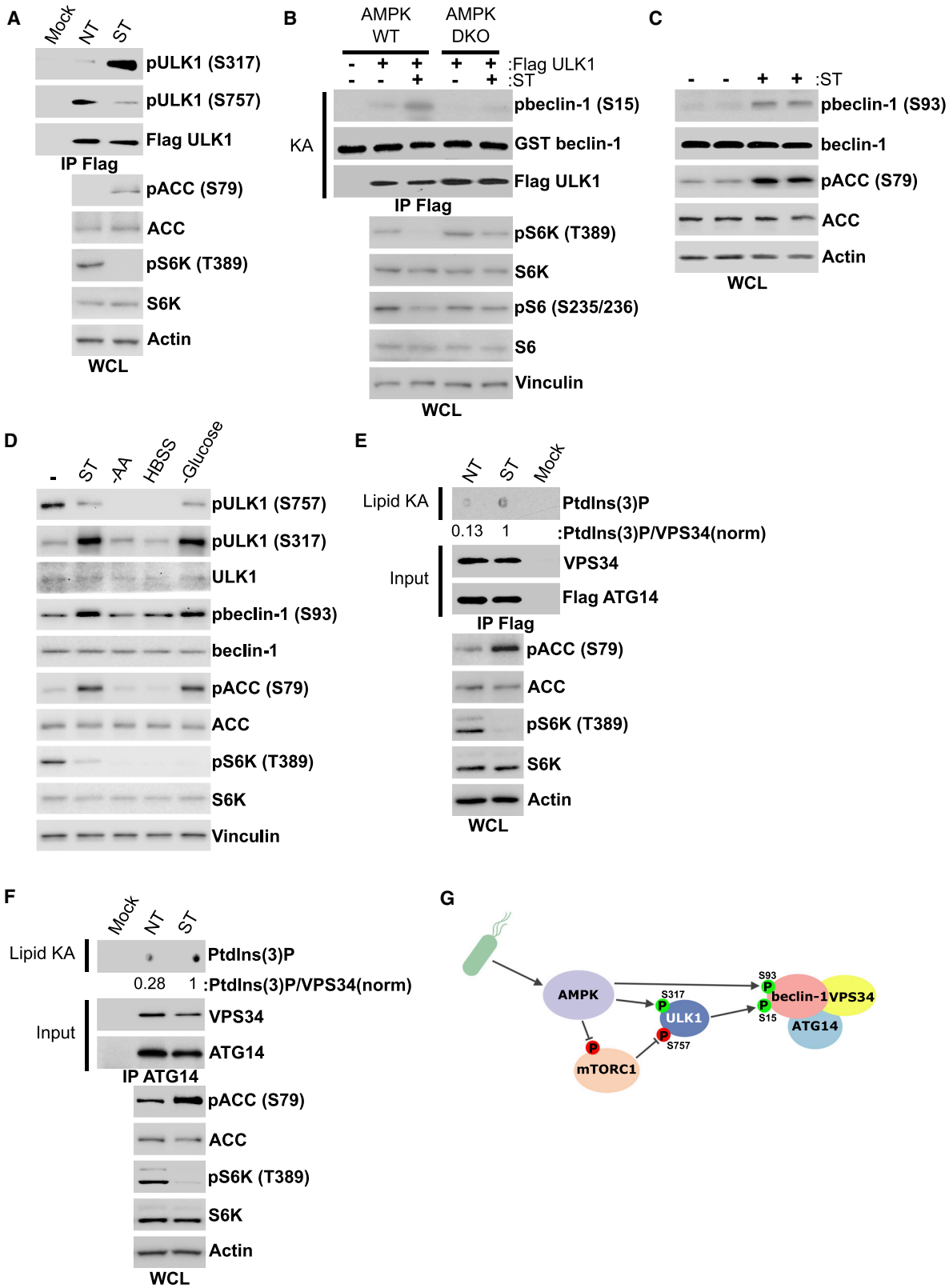

(legend on next page)

Detection of Pathogen-Derived Outer Membrane Vesicles Promotes AMPK Activation

We next sought to determine the mechanism by which the host cell detects *Salmonella* and activates AMPK. Mammalian cells have several pathogen recognition receptors (PRRs), which are capable of detecting a range of bacterial macromolecules and activating the host immune response (Mishra et al., 2017). The best characterized of these receptors are the Toll-like receptors (TLRs), which are capable of detecting lipopolysaccharides (LPSs), bacterial DNA, or bacterial proteins, including flagellin (Takeuchi and Akira, 2010). To determine whether the activation of TLRs was required for AMPK upregulation in response to extracellular bacteria, we activated TLR receptors with LPSs, R848 (resiquimod), and murine norovirus 1 (MNV1) that activate TLR4, TLR7/8, and TLR3/7/8, respectively (Dammermann et al., 2013). Analysis of AMPK activation by western blot clearly showed that TLR ligands and MNV1 were not capable of activating AMPK signaling (Figure 5A). Next, we attempted to activate the host response with an unbiased approach for bacterial antigens by treating cells with *Salmonella* that were killed by paraformaldehyde fixation to preserve bacterial PAMPs (pathogen-associated molecular patterns). We observed that fixed bacteria were unable to activate AMPK or inhibit mTORC1 (Figure 5B), indicating that viable bacteria are required to stimulate AMPK-mediated signaling to the autophagy kinases.

Upon re-analysis of our immunofluorescent images, we noted that cells that did not contain bacteria still stained positive for small LPS puncta, which were not present in the untreated samples (Figure S5A). We hypothesized that these small puncta may be *Salmonella*-derived outer membrane vesicles (OMVs). OMVs are produced by the budding of the outer membrane of Gram-negative bacteria, which contain a diverse array of periplasmic cargo, including proteins, nucleic acids, lipids, and small molecules (Kulkarni and Jagannadham, 2014). Pathogenic bacteria have also been described to deliver virulence factors to cells via OMVs, and *Salmonella* has been shown to selectively load OMVs with different cargo, depending on environmental stimuli (Bai et al., 2014). OMV production is independent of the T3SS and requires viable bacteria, which is consistent with the retention of AMPK activation in the T3SS mutant *Salmonella* and the failure of paraformaldehyde-inactivated *Salmonella* to activate signaling to the autophagy pathway. Therefore, we next sought to determine directly whether *Salmonella* OMVs were responsible for AMPK activation by extracellular bacteria. OMVs from *Salmonella* were purified using a combination of established protocols, which included filtration, polyethylene glycol enrichment, and ultracentrifugation (Bai et al., 2014; Rider et al., 2016). Purified OMVs were analyzed by laser scatter microscopy, were found to have an average diameter of 140 nm, and were free of intact bacteria (Figure 5C). We next sought to determine whether our purified OMVs were capable of entering mammalian cells and whether OMVs produced during our standard *Salmonella* infection protocol were entering the cell. Using sequential staining against *Salmonella* LPS (pre- and post-permabilization) we observed that OMVs were entering the cells during *Salmonella* infection or using our purified fraction (Figures 5D and S5B). We then treated cells with *Salmonella* or OMVs and analyzed AMPK activation and OMV entry by immunofluorescence and found that OMV treatment was sufficient to activate AMPK (Figures 5E and S5C). Next, AMPK activation and mTORC1 inhibition were analyzed by western blot after treatment with *Salmonella* or purified OMVs. We observed that OMV treatment triggered both AMPK activation and mTORC1 inhibition (Figure 5F). In addition, we found that OMVs purified from InvA mutant *Salmonella* are also capable of inducing AMPK and mTORC1 signaling (Figure S5D). These data show that AMPK signaling is induced by *Salmonella*-derived OMVs, which can occur independently of bacterial invasion.

The entry of OMVs into host cells has been described through multiple entry points in mammalian cells (O'Donoghue and Krachler, 2016). To determine whether OMV uptake was required for AMPK signaling, we infected cells in the presence or absence of either filipin III or dynasore, which are reported to inhibit some routes of OMV entry. We observed that filipin III activates AMPK independently of infection, while dynasore fails to block OMV entry in cells treated with either OMV or *Salmonella*, precluding their use for our study (Figures S5E and S5F). However, we found that the fixation of OMVs by paraformaldehyde followed by stringent washing prevents entry without disrupting the integrity of the OMVs (Figure S5G). We then treated

Figure 4. *Salmonella*-Mediated Stimulation of AMPK Activates Autophagy Kinases ULK1 and VPS34

(A) HEK293A cells stably expressing FLAG-ULK1 were infected with *Salmonella* for 1 h, followed by FLAG-ULK1 pull-down. AMPK-mediated activation (S317) and mTORC1-mediated inhibition (S757) of ULK1 were examined by western blot.

(B) AMPK wild-type and AMPK α1/2 knockout MEF cells transfected with FLAG-ULK1 were treated with or without *Salmonella* for 1 h, followed by FLAG-ULK1 pull-down. An *in vitro* kinase assay was then performed using bacterially purified beclin-1, a known downstream target of ULK1, as substrate. ULK1 activity was then determined by measuring the phosphorylation of beclin-1 at S15.

(C) HCT116 cells were infected with *Salmonella* for 1 h in duplicate. AMPK-mediated phosphorylation of the VPS34 subunit beclin-1 at S93 was determined by western blot.

(D) MEF cells were treated with either full medium, *Salmonella*, amino acid starvation medium, HBSS, or glucose deprivation medium for 1 h. The regulation of ULK1 and the VPS34 subunit beclin-1 was determined by western blot.

(E) HEK293A cells transfected with FLAG-ATG14 were treated with or without *Salmonella* for 1 h, followed by FLAG-ATG14 pull-down. The activity of ATG14-containing VPS34 complexes was analyzed by an *in vitro* lipid kinase assay and dot-blot assay blotting for PtdIns(3)P. Whole-cell lysates were immunoblotted for the analysis of AMPK and mTORC1 signaling.

(F) HEK293A wild-type cells were treated with or without *Salmonella* for 1 h, followed by the immunoprecipitation of endogenous ATG14. The activity of ATG14-containing VPS34 complexes was analyzed by an *in vitro* lipid kinase assay and a dot-blot assay, as described above. Whole-cell lysates were immunoblotted for the analysis of AMPK and mTORC1 signaling.

(G) Model of AMPK-mediated activation of autophagy kinases upon detection of *Salmonella*.

Unless otherwise indicated, experiments were performed three times.

See also Figure S4.

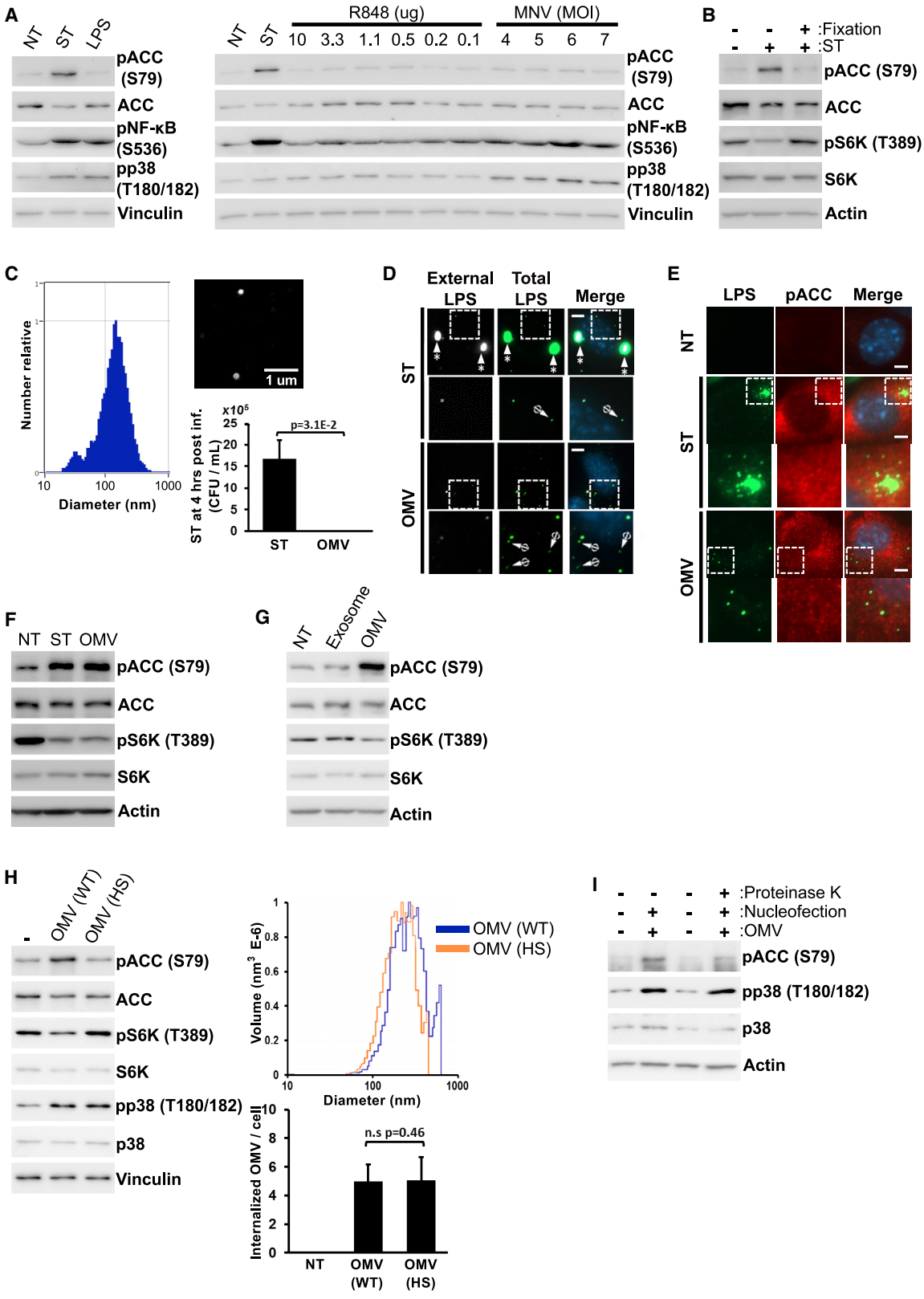

(legend on next page)

cells with either control or fixed OMVs and analyzed downstream signaling. The fixation of OMVs resulted in a profound loss in AMPK activation, indicating that OMV entry is required for the detection and activation of the autophagy pathway (Figure S5G). Membrane disruption caused by *Salmonella* infection has been described as resulting in amino acid loss and mTORC1 inhibition (Tattoli et al., 2012b). Therefore, we attempted to examine whether OMV-mediated membrane perturbation contributed to the regulation of AMPK and mTORC1. Using digitonin at previously reported concentrations for studying the effects of pathogen-induced membrane disruption, we observed a decrease in membrane integrity (Tattoli et al., 2012b), as measured by trypan blue uptake, and alterations in AMPK and mTORC1 signaling (Figure S5H). However, OMV treatment did not increase membrane permeability, indicating that OMVs may not induce stress signaling through the disruption of the plasma membrane (Figure S5H). We next reasoned that if stress signaling was due to a milder level of membrane disruption, then exosomes, mammalian-derived secretory vesicles of similar size, should also activate AMPK. Therefore, we added an equal number of *Salmonella*-derived OMVs and neuron-derived exosomes to cells and analyzed AMPK and mTORC1 signaling. We observed that OMVs but not exosomes were capable of activating AMPK, which strongly indicates that AMPK and mTORC1 regulation is not a result of membrane perturbation (Figure 5G).

Next, to identify the PRRs responsible for AMPK activation, we knocked out genes using the CRISPR-Cas9 involved in detecting pathogenic macromolecules and activating the host immune response, including IRAK, TRAF6, NOD1, NOD2, and STING. However, we observed no difference in AMPK regulation in the knockout cell lines compared to the *wild-type* when exposed to *Salmonella* or OMVs, which may suggest that signaling can be stimulated by more than one PAMP or sensed by more than one PRR (Figures S5I–S5K). We next attempted to examine the biological properties of OMV-derived PAMPs involved in AMPK signaling. We treated OMVs with a mild heat shock followed by rapid cooling to denature proteins (55°C) and observed that the heat-shocked OMVs are incapable of inducing AMPK signaling, even though they retained their structural integrity and the majority of their cargo (Figures 5H and S5L). The loss of AMPK activation by mild heat shock indicates that the PAMP or PAMPs responsible may be protein, which has denatured under these conditions. To directly test whether the OMV-derived PAMP was a protein, we introduced proteinase K into OMVs by electroporation and tested their ability to activate AMPK. We found that OMVs electroporated with buffer alone maintained normal signaling, indicating that the electroporation itself did not affect OMV detection (Figure 5I). However, we observed that proteinase K treatment resulted in a reduction in AMPK activation (Figure 5I). Our data strongly indicate that protein or proteins from the OMVs are responsible for inducing AMPK signaling.

AMPK Signaling Promotes Xenophagy

A key prediction from our model linking *Salmonella*-induced AMPK signaling to the activation of the xenophagic response is that cells lacking AMPK activity should have a reduction in the autophagic capture of internalized *Salmonella.* To test this hypothesis and determine the biological contribution of AMPK signaling to the promotion of xenophagy, we quantified *Salmonella* incorporation into $LC3B^+$ vesicles in AMPK wild-type and deficient MEF. Unbiased quantification of $LC3B^+$ internalized bacteria was achieved using the blinded application of Volocity program object detection from immunofluorescent images of triple stained for external bacteria (anti-LPS before permeabilization), total bacteria (anti-LPS after permeabilization), and $LC3B^+$ puncta (Figure S6). In agreement with our prediction, we observed a reduction in the number of $LC3B^+$ internalized *Salmonella* in the AMPK double-knockout background (Figure 6A). To determine whether the increase in $LC3B^+$ bacteria is a result of increased capture by autophagy or LAP, we repeated the experiment using the same triple-staining technique detailed above, substituting LC3B for p62. p62 is reported not to localize

Figure 5. Pathogen-Derived Outer Membrane Vesicles Stimulate AMPK Activation

(A) MEF cells were treated with *Salmonella*, lipopolysaccharides ([LPSs] 2 μg/mL), resiquimod (R848, indicated concentrations), and murine noroviruses ([MNVs] indicated MOI) for 1 h. Whole-cell lysates were immunoblotted using the antibodies indicated.

(B) MEF cells were infected with either *Salmonella* (wild-type) or paraformaldehyde (PFA)-treated *Salmonella* for 1 h. Whole-cell lysates were immunoblotted for AMPK and mTORC1 activities using the antibodies indicated.

(C) Purified OMVs were analyzed by ZetaView Nanoparticle Tracking Analysis showing the distribution of OMV particle size (left) and showing a representative image of OMV particles (center). OMVs were confirmed to be free of intact bacteria via CFU assays (right).

(D) MEF cells were treated with *Salmonella* or purified OMVs (unless otherwise stated, 3.6×10^{10} particles/mL were added) for 1 h. External and total LPS were stained to highlight internalized OMVs and analyzed by immunofluorescence (scale bars, 5 μM). Arrows with ϕ indicate internalized OMVs. Arrowheads with * indicate external *Salmonella.*

(E) MEF cells were treated with *Salmonella* or purified OMVs for 1 h. AMPK-mediated phosphorylation of ACCs and LPSs were stained and analyzed by immunofluorescence. Scale bars, 5 μM.

(F) MEF cells were treated with either *Salmonella* or purified OMVs for 1 h. Whole-cell lysate was immunoblotted for the activities of AMPK and mTORC1.

(G) MEF cells were treated with either purified exosomes or OMVs for 1 h. Whole-cell lysate was immunoblotted for the analysis of AMPK and mTORC1 signaling.

(H) MEF cells were treated with either wild-type OMVs or 55°C-treated OMVs for 1 h. Whole-cell lysates were immunoblotted using the antibodies indicated (top left). Heat-treated OMVs were analyzed by laser scattering microscopy, and a graph generated by ZetaView Nanoparticle Tracking Analysis compares the size distribution of wild-type and heat-treated OMV particles (top right). OMV internalization rates were quantified by immunofluorescence (bottom).

(I) Proteinase K was inserted into OMVs via nucleofection. OMVs were repelleted and excess proteinase K removed by three washes of OMV pellets. MEF cells were then treated with control nucleofected OMVs or proteinase K-containing OMVs for 1 h. Whole-cell lysates were immunoblotted using the antibodies indicated.

Unless otherwise indicated, experiments were performed three times. Data are represented as means ± SDs, and p values were determined by Student's t test. See also Figure S5.

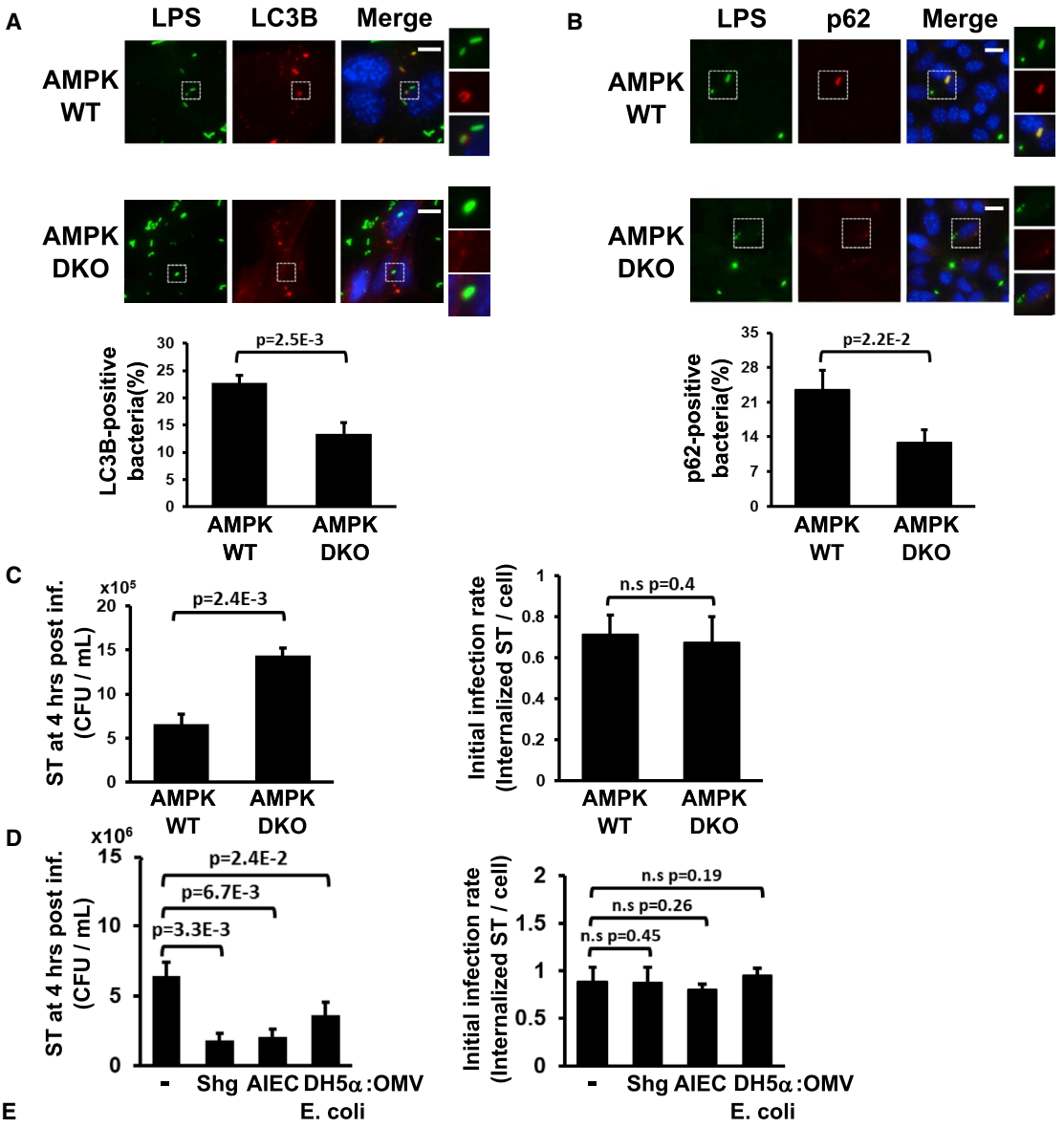

(legend on next page)

to LAP vesicles (Lam et al., 2013) and is an established marker of bacteria that are targeted for autophagic degradation (Wild et al., 2011). Quantification of p62$^+$ *Salmonella* showed a marked defect in the efficiency of AMPK-deficient cells in the targeting of *Salmonella* to p62$^+$ structures that was similar to the reduction observed from LC3B co-staining (Figure 6B), indicating a defect in xenophagy in AMPK-deficient cells. Notably, LC3B and p62$^+$ *Salmonella* were still observable in the AMPK double-knockout cells, indicating that AMPK-independent xenophagy pathways are still functioning. These pathways could include selective autophagy pathways that recognize ubiquitinated bacteria or damaged SCV, neither of which have been previously linked to AMPK. However, the presence of increased *Salmonella* in the AMPK-deficient cells clearly indicate a role for AMPK in promoting the xenophagic response.

Next, to confirm that AMPK signaling promotes xenophagy, we infected AMPK wild-type and deficient MEFs with *Salmonella* and performed a colony-forming unit (CFU) assay. Consistent with our previous data, we found that AMPK-deficient cells had significantly higher numbers of internalized bacteria at 4 h post-infection than AMPK wild-type cells, despite both lines starting out with an equal rate of infection (Figure 6C). Lastly, we wished to examine whether AMPK activation is triggered by OMVs from other Gram-negative bacteria, both infectious and non-infectious, and whether it could enhance the xenophagy rate of *Salmonella*. We found that 4 h post-infection, priming with OMVs purified from *Shigella*, AIEC, or DH5α *E. coli* promotes bacterial clearance compared to samples without OMVs pre-incubation (Figure 6D). Our data indicate that OMV-stimulated AMPK signaling plays an important role in the autophagic suppression of invading *Salmonella* (Figure 6E).

DISCUSSION

As part of the innate immune system, xenophagy plays a key role in the restriction of intracellular bacterial growth. Here, we describe a signaling pathway that promotes xenophagy through AMPK-dependent activation of autophagy kinases. This early activation of the autophagy pathway can be stimulated by OMVs shed by Gram-negative bacteria, independent of bacterial invasion and internalization. We observed that the detection of extracellular bacteria resulted in the regulation of AMPK and mTORC1 activity, as well as an activation of autophagy kinase complexes, but it did not lead to an increase in bulk autophagy.

While we do not yet have the full picture of how autophagy is inhibited downstream of mTORC1 in response to *Salmonella,* the potential benefits to the cell are more obvious. Autophagy has a tremendous degradative capacity, capable of turning over up to 3% of total cellular proteins per hour when mTORC1 is inhibited by amino acid withdrawal (Mizushima and Klionsky, 2007). If every cell that encountered pathogens, especially those never destined to be infected, began indiscriminate degradation of their cytoplasm, then this would be an enormously wasteful and inefficient way to target pathogens for clearance. Instead, we have found that the cell has developed a sophisticated method using AMPK signaling to selectively prime the autophagy pathway for the clearance of pathogens even before the bacteria have a chance to enter the cell.

Several studies have shown that once *Salmonella* is internalized, there are many events that contribute to bacterial capture by the autophagosome, including but not limited to targeting of damaged membranes, transient loss of nutrients, and the ubiquitination of bacterial proteins (Gomes and Dikic, 2014; Chauhan et al., 2015; Tattoli et al., 2012b). Here, we showed that AMPK signaling not only pre-activates the ULK1 and VPS34 kinase complexes but is also required for efficient xenophagy induction. Therefore, it will be of interest in future studies to determine whether or how activation of the ULK1 and VPS34 kinase complexes is important for specific events associated with bacterial capture by autophagosomes.

The demonstration that OMVs are capable of evoking signaling responses that have previously been attributed to cellular damage caused by bacterial invasion was unexpected. Therefore, it will be interesting to determine whether other autophagy-related aspects of the innate immune response may be similarly affected by OMV detection. For example, autophagy proteins have been described as influencing the secretion of inflammatory cytokines (Sorbara et al., 2013). It would be interesting to see whether OMV-mediated activation of the autophagy pathway plays a role in the regulation of the inflammatory response.

Finally, OMVs from infectious bacteria have also been described as harboring virulence factors that can enhance pathogenicity (Sorbara et al., 2013). Therefore, one may imagine that there is a trade-off for the bacteria in which OMV production will lead to the activation of xenophagy but also act as a vehicle to deliver factors that will promote growth. In the course of this study, we observed several instances in which internalized bacteria were surrounded by OMVs, and these bacteria were seldom targeted by autophagosomes. The Red Queen race between

Figure 6. AMPK Promotes Xenophagy Induction in Response to Bacterial Infection

(A and B) AMPK wild-type and α1/2 knockout MEF cells were infected with *Salmonella* for 1 h (unless otherwise stated, an MOI of 180 was used) in the presence of 0.2 μM bafilomycin A1. Bacteria were stained using anti-LPS antibodies to analyze localization in addition to the autophagy markers LC3B (A) and p62 (B) (scale bars, 10 μM for A and 20 μM for B). Quantification of bacteria undergoing autophagic clearance is demonstrated at bottom. Experiments were performed twice.

(C) AMPK wild-type and α1/2 knockout MEF cells were infected with *Salmonella* for 1 h. Xenophagy rates were examined through CFU assays. Quantification of infection rates by immunofluorescence is demonstrated at right.

(D) MEF cells were infected with *Salmonella* in the absence or presence of OMV purified from *Shigella*, AIEC, or DH5α *E. coli* for 1 h. Xenophagy rates were examined through CFU assays. Initial infection rates were quantified by immunofluorescence and is shown at right.

(E) A working model of AMPK signaling through ULK1-VPS34 complexes in response to *Salmonella* infection.

Unless otherwise indicated, experiments were performed three times. Data are represented as means ± SDs, and p values were determined by Student's t test. See also Figure S6.

host and pathogen makes it quite likely that *Salmonella* and other Gram-negative bacteria have already developed measures designed to circumvent or exploit the detection of OMVs, and the characterization of this potential interplay warrants further investigation.

STAR★METHODS

Detailed methods are provided in the online version of this paper and include the following:

- KEY RESOURCES TABLE
- CONTACT FOR REAGENT AND RESOURCE SHARING
- EXPERIMENTAL MODEL AND SUBJECT DETAILS
  - Cell Culture
  - Generation of Stable Cell Line
  - Generation of knock-out cell lines using CRISPR/Cas9
- METHOD DETAILS
  - Bacterial Infection
  - Preparation of bacterial supernatant
  - OMV Purification
  - OMV modifications
  - Western blot and Immunoprecipitation
  - Immunofluorescence
  - *In vitro* ULK1 Kinase Assay
  - *In vitro* VPS34 Lipid Kinase Assay
  - Colony Forming Unit (CFU) Assay
- QUANTIFICATION AND STATISTICAL ANALYSIS
  - Quantification of Immunofluorescence
  - Statistical Analysis

SUPPLEMENTAL INFORMATION

Supplemental Information can be found with this article online at https://doi.org/10.1016/j.celrep.2019.01.062.

ACKNOWLEDGMENTS

We would like to thank members of the Russell laboratory for advice and critical reading of this manuscript, Dr. Russell Jones (McGill University) for supplying the AMPK α1/2 double-knockout MEFs, and Stephen Girardin for NOD1 and NOD2 knockout lines. The authors would like to apologize to the colleagues whose significant work could not be included due to length, citation limitations, or author oversight. This work was supported by Canadian Institutes of Health Research (CIHR) Project Grants awarded to R.C.R. (PJT153034) and M.D.F. (PJT148634). M.D.F. is also supported by a CIHR New Investigator Award (MSH141981). Instrumentation for OMV and exosome analysis was supported by an NSERC Research Tools and Instruments grant to D.J.G.

AUTHOR CONTRIBUTIONS

T.T.L., O.C.M.-M., and R.C.R. wrote the manuscript. M.D.F., D.J.G., F.-X.C.-V., and S.S. assisted in manuscript preparation and experimental planning and generated cell lines and reagents for the study. T.T.L., M.A., O.C.M.-M., and R.C.R. designed the research and interpreted the data. The majority of data was generated by T.T.L., M.A., and O.C.M. N.D.L. harvested and differentiated all of the BMDMs used in the study. R.M.A. generated the data on TLR signaling. Y.S. generated the data on the heat shock of OMV. Z.G. generated the data on ULK1 localization. R.R. assisted in exosome production and OMV characterization.

DECLARATION OF INTERESTS

The authors declare no competing interests.

Received: May 14, 2018
Revised: December 14, 2018
Accepted: January 16, 2019
Published: February 19, 2019

REFERENCES

Bai, J., Kim, S.I., Ryu, S., and Yoon, H. (2014). Identification and characterization of outer membrane vesicle-associated proteins in Salmonella enterica serovar Typhimurium. Infect. Immun. *82*, 4001–4010.

Boyle, K.B., and Randow, F. (2013). The role of 'eat-me' signals and autophagy cargo receptors in innate immunity. Curr. Opin. Microbiol. *16*, 339–348.

Campbell-Valois, F.X., Sachse, M., Sansonetti, P.J., and Parsot, C. (2015). Escape of Actively Secreting Shigella flexneri from ATG8/LC3-Positive Vacuoles Formed during Cell-To-Cell Spread Is Facilitated by IcsB and VirA. MBio *6*, e02567–e025614.

Chauhan, S., Mandell, M.A., and Deretic, V. (2015). IRGM governs the core autophagy machinery to conduct antimicrobial defense. Mol. Cell *58*, 507–521.

Cirillo, D.M., Valdivia, R.H., Monack, D.M., and Falkow, S. (1998). Macrophage-dependent induction of the Salmonella pathogenicity island 2 type III secretion system and its role in intracellular survival. Mol. Microbiol. *30*, 175–188.

Dammermann, W., Wollenberg, L., Bentzien, F., Lohse, A., and Lüth, S. (2013). Toll like receptor 2 agonists lipoteichoic acid and peptidoglycan are able to enhance antigen specific IFNγ release in whole blood during recall antigen responses. J. Immunol. Methods *396*, 107–115.

Egan, D.F., Shackelford, D.B., Mihaylova, M.M., Gelino, S., Kohnz, R.A., Mair, W., Vasquez, D.S., Joshi, A., Gwinn, D.M., Taylor, R., et al. (2011). Phosphorylation of ULK1 (hATG1) by AMP-activated protein kinase connects energy sensing to mitophagy. Science *331*, 456–461.

Galán, J.E., and Curtiss, R., 3rd. (1989). Cloning and molecular characterization of genes whose products allow Salmonella typhimurium to penetrate tissue culture cells. Proc. Natl. Acad. Sci. USA *86*, 6383–6387.

Galán, J.E., and Curtiss, R., 3rd. (1991). Distribution of the invA, -B, -C, and -D genes of Salmonella typhimurium among other Salmonella serovars: invA mutants of Salmonella typhi are deficient for entry into mammalian cells. Infect. Immun. *59*, 2901–2908.

Galic, S., Fullerton, M.D., Schertzer, J.D., Sikkema, S., Marcinko, K., Walkley, C.R., Izon, D., Honeyman, J., Chen, Z.P., van Denderen, B.J., et al. (2011). Hematopoietic AMPK β1 reduces mouse adipose tissue macrophage inflammation and insulin resistance in obesity. J. Clin. Invest. *121*, 4903–4915.

Ganesan, R., Hos, N.J., Gutierrez, S., Fischer, J., Stepek, J.M., Daglidu, E., Krönke, M., and Robinson, N. (2017). Salmonella Typhimurium disrupts Sirt1/AMPK checkpoint control of mTOR to impair autophagy. PLoS Pathog. *13*, e1006227.

Ganley, I.G., Lam, H., Wang, J., Ding, X., Chen, S., and Jiang, X. (2009). ULK1.ATG13.FIP200 complex mediates mTOR signaling and is essential for autophagy. J. Biol. Chem. *284*, 12297–12305.

Gaudet, R.G., Guo, C.X., Molinaro, R., Kottwitz, H., Rohde, J.R., Dangeard, A.S., Arrieumerlou, C., Girardin, S.E., and Gray-Owen, S.D. (2017). Innate Recognition of Intracellular Bacterial Growth Is Driven by the TIFA-Dependent Cytosolic Surveillance Pathway. Cell Rep. *19*, 1418–1430.

Gomes, L.C., and Dikic, I. (2014). Autophagy in antimicrobial immunity. Mol. Cell *54*, 224–233.

Grégoire, I.P., Richetta, C., Meyniel-Schicklin, L., Borel, S., Pradezynski, F., Diaz, O., Deloire, A., Azocar, O., Baguet, J., Le Breton, M., et al. (2011). IRGM is a common target of RNA viruses that subvert the autophagy network. PLoS Pathog. *7*, e1002422.

Gwinn, D.M., Shackelford, D.B., Egan, D.F., Mihaylova, M.M., Mery, A., Vasquez, D.S., Turk, B.E., and Shaw, R.J. (2008). AMPK phosphorylation of raptor mediates a metabolic checkpoint. Mol. Cell *30*, 214–226.

Hawley, S.A., Fullerton, M.D., Ross, F.A., Schertzer, J.D., Chevtzoff, C., Walker, K.J., Peggie, M.W., Zibrova, D., Green, K.A., Mustard, K.J., et al. (2012). The ancient drug salicylate directly activates AMP-activated protein kinase. Science *336*, 918–922.

Hensel, M., Shea, J.E., Gleeson, C., Jones, M.D., Dalton, E., and Holden, D.W. (1995). Simultaneous identification of bacterial virulence genes by negative selection. Science *269*, 400–403.

Hosokawa, N., Hara, T., Kaizuka, T., Kishi, C., Takamura, A., Miura, Y., Iemura, S., Natsume, T., Takehana, K., Yamada, N., et al. (2009). Nutrient-dependent mTORC1 association with the ULK1-Atg13-FIP200 complex required for autophagy. Mol. Biol. Cell *20*, 1981–1991.

Huang, J., and Brumell, J.H. (2014). Bacteria-autophagy interplay: a battle for survival. Nat. Rev. Microbiol. *12*, 101–114.

Huang, J., Canadien, V., Lam, G.Y., Steinberg, B.E., Dinauer, M.C., Magalhaes, M.A., Glogauer, M., Grinstein, S., and Brumell, J.H. (2009). Activation of antibacterial autophagy by NADPH oxidases. Proc. Natl. Acad. Sci. USA *106*, 6226–6231.

Huett, A., Heath, R.J., Begun, J., Sassi, S.O., Baxt, L.A., Vyas, J.M., Goldberg, M.B., and Xavier, R.J. (2012). The LRR and RING domain protein LRSAM1 is an E3 ligase crucial for ubiquitin-dependent autophagy of intracellular Salmonella Typhimurium. Cell Host Microbe *12*, 778–790.

Itakura, E., and Mizushima, N. (2010). Characterization of autophagosome formation site by a hierarchical analysis of mammalian Atg proteins. Autophagy *6*, 764–776.

Jung, C.H., Jun, C.B., Ro, S.H., Kim, Y.M., Otto, N.M., Cao, J., Kundu, M., and Kim, D.H. (2009). ULK-Atg13-FIP200 complexes mediate mTOR signaling to the autophagy machinery. Mol. Biol. Cell *20*, 1992–2003.

Katpally, U., Wobus, C.E., Dryden, K., Virgin, H.W.T., 4th, and Smith, T.J. (2008). Structure of antibody-neutralized murine norovirus and unexpected differences from viruslike particles. J. Virol. *82*, 2079–2088.

Kaur, J., and Debnath, J. (2015). Autophagy at the crossroads of catabolism and anabolism. Nat. Rev. Mol. Cell Biol. *16*, 461–472.

Kim, J., Kundu, M., Viollet, B., and Guan, K.L. (2011). AMPK and mTOR regulate autophagy through direct phosphorylation of Ulk1. Nat. Cell Biol. *13*, 132–141.

Kim, J., Kim, Y.C., Fang, C., Russell, R.C., Kim, J.H., Fan, W., Liu, R., Zhong, Q., and Guan, K.L. (2013). Differential regulation of distinct Vps34 complexes by AMPK in nutrient stress and autophagy. Cell *152*, 290–303.

Kulkarni, H.M., and Jagannadham, M.V. (2014). Biogenesis and multifaceted roles of outer membrane vesicles from Gram-negative bacteria. Microbiology *160*, 2109–2121.

Lam, G.Y., Cemma, M., Muise, A.M., Higgins, D.E., and Brumell, J.H. (2013). Host and bacterial factors that regulate LC3 recruitment to Listeria monocytogenes during the early stages of macrophage infection. Autophagy *9*, 985–995.

Li, S., Wandel, M.P., Li, F., Liu, Z., He, C., Wu, J., Shi, Y., and Randow, F. (2013). Sterical hindrance promotes selectivity of the autophagy cargo receptor NDP52 for the danger receptor galectin-8 in antibacterial autophagy. Sci. Signal. *6*, ra9.

Martinez, J., Almendinger, J., Oberst, A., Ness, R., Dillon, C.P., Fitzgerald, P., Hengartner, M.O., and Green, D.R. (2011). Microtubule-associated protein 1 light chain 3 alpha (LC3)-associated phagocytosis is required for the efficient clearance of dead cells. Proc. Natl. Acad. Sci. USA *108*, 17396–17401.

Martinez, J., Malireddi, R.K., Lu, Q., Cunha, L.D., Pelletier, S., Gingras, S., Orchard, R., Guan, J.L., Tan, H., Peng, J., et al. (2015). Molecular characterization of LC3-associated phagocytosis reveals distinct roles for Rubicon, NOX2 and autophagy proteins. Nat. Cell Biol. *17*, 893–906.

Mishra, A., Akhtar, S., Jagannath, C., and Khan, A. (2017). Pattern recognition receptors and coordinated cellular pathways involved in tuberculosis immunopathogenesis: Emerging concepts and perspectives. Mol. Immunol. *87*, 240–248.

Mizushima, N., and Klionsky, D.J. (2007). Protein turnover via autophagy: implications for metabolism. Annu. Rev. Nutr. *27*, 19–40.

Nazio, F., Strappazzon, F., Antonioli, M., Bielli, P., Cianfanelli, V., Bordi, M., Gretzmeier, C., Dengjel, J., Piacentini, M., Fimia, G.M., and Cecconi, F. (2013). mTOR inhibits autophagy by controlling ULK1 ubiquitylation, self-association and function through AMBRA1 and TRAF6. Nat. Cell Biol. *15*, 406–416.

O'Donoghue, E.J., and Krachler, A.M. (2016). Mechanisms of outer membrane vesicle entry into host cells. Cell. Microbiol. *18*, 1508–1517.

Ochman, H., Soncini, F.C., Solomon, F., and Groisman, E.A. (1996). Identification of a pathogenicity island required for Salmonella survival in host cells. Proc. Natl. Acad. Sci. USA *93*, 7800–7804.

Owen, K.A., Meyer, C.B., Bouton, A.H., and Casanova, J.E. (2014). Activation of focal adhesion kinase by Salmonella suppresses autophagy via an Akt/mTOR signaling pathway and promotes bacterial survival in macrophages. PLoS Pathog. *10*, e1004159.

Park, J.M., Jung, C.H., Seo, M., Otto, N.M., Grunwald, D., Kim, K.H., Moriarity, B., Kim, Y.M., Starker, C., Nho, R.S., et al. (2016). The ULK1 complex mediates MTORC1 signaling to the autophagy initiation machinery via binding and phosphorylating ATG14. Autophagy *12*, 547–564.

Rider, M.A., Hurwitz, S.N., and Meckes, D.G., Jr. (2016). ExtraPEG: A Polyethylene Glycol-Based Method for Enrichment of Extracellular Vesicles. Sci. Rep. *6*, 23978.

Russell, R.C., Tian, Y., Yuan, H., Park, H.W., Chang, Y.Y., Kim, J., Kim, H., Neufeld, T.P., Dillin, A., and Guan, K.L. (2013). ULK1 induces autophagy by phosphorylating Beclin-1 and activating VPS34 lipid kinase. Nat. Cell Biol. *15*, 741–750.

Russell, R.C., Yuan, H.X., and Guan, K.L. (2014). Autophagy regulation by nutrient signaling. Cell Res. *24*, 42–57.

Sad, S., Dudani, R., Gurnani, K., Russell, M., van Faassen, H., Finlay, B., and Krishnan, L. (2008). Pathogen proliferation governs the magnitude but compromises the function of CD8 T cells. J. Immunol. *180*, 5853–5861.

Sanjuan, M.A., Dillon, C.P., Tait, S.W., Moshiach, S., Dorsey, F., Connell, S., Komatsu, M., Tanaka, K., Cleveland, J.L., Withoff, S., and Green, D.R. (2007). Toll-like receptor signalling in macrophages links the autophagy pathway to phagocytosis. Nature *450*, 1253–1257.

Shaw, R.J., Bardeesy, N., Manning, B.D., Lopez, L., Kosmatka, M., DePinho, R.A., and Cantley, L.C. (2004). The LKB1 tumor suppressor negatively regulates mTOR signaling. Cancer Cell *6*, 91–99.

Small, C.L., Reid-Yu, S.A., McPhee, J.B., and Coombes, B.K. (2013). Persistent infection with Crohn's disease-associated adherent-invasive Escherichia coli leads to chronic inflammation and intestinal fibrosis. Nat. Commun. *4*, 1957.

Sorbara, M.T., Ellison, L.K., Ramjeet, M., Travassos, L.H., Jones, N.L., Girardin, S.E., and Philpott, D.J. (2013). The protein ATG16L1 suppresses inflammatory cytokines induced by the intracellular sensors Nod1 and Nod2 in an autophagy-independent manner. Immunity *39*, 858–873.

Takeuchi, O., and Akira, S. (2010). Pattern recognition receptors and inflammation. Cell *140*, 805–820.

Tattoli, I., Philpott, D.J., and Girardin, S.E. (2012a). The bacterial and cellular determinants controlling the recruitment of mTOR to the Salmonella-containing vacuole. Biol. Open *1*, 1215–1225.

Tattoli, I., Sorbara, M.T., Vuckovic, D., Ling, A., Soares, F., Carneiro, L.A., Yang, C., Emili, A., Philpott, D.J., and Girardin, S.E. (2012b). Amino acid starvation induced by invasive bacterial pathogens triggers an innate host defense program. Cell Host Microbe *11*, 563–575.

Thurston, T.L., Wandel, M.P., von Muhlinen, N., Foeglein, A., and Randow, F. (2012). Galectin 8 targets damaged vesicles for autophagy to defend cells against bacterial invasion. Nature *482*, 414–418.

Wild, P., Farhan, H., McEwan, D.G., Wagner, S., Rogov, V.V., Brady, N.R., Richter, B., Korac, J., Waidmann, O., Choudhary, C., et al. (2011).

Phosphorylation of the autophagy receptor optineurin restricts Salmonella growth. Science *333*, 228–233.

Yuan, H.X., Russell, R.C., and Guan, K.L. (2013). Regulation of PIK3C3/VPS34 complexes by MTOR in nutrient stress-induced autophagy. Autophagy *9*, 1983–1995.

Zheng, Y.T., Shahnazari, S., Brech, A., Lamark, T., Johansen, T., and Brumell, J.H. (2009). The adaptor protein p62/SQSTM1 targets invading bacteria to the autophagy pathway. J. Immunol. *183*, 5909–5916.

Zhou, G., Myers, R., Li, Y., Chen, Y., Shen, X., Fenyk-Melody, J., Wu, M., Ventre, J., Doebber, T., Fujii, N., et al. (2001). Role of AMP-activated protein kinase in mechanism of metformin action. J. Clin. Invest. *108*, 1167–1174.

STAR★METHODS

KEY RESOURCES TABLE

REAGENT or RESOURCE	SOURCE	IDENTIFIER
Antibodies		
Rabbit monoclonal anti-PtdIns(3)P	Millennium Pharmaceuticals	N/A
Rabbit monoclonal anti-beclin-1	Cell Signaling Technology	Cat#3495; RRID: AB_1903911
Rabbit monoclonal anti-phospho-beclin-1 S15 (clone D4B7R)	Cell Signaling Technology	Cat#84966
Rabbit monoclonal anti-phospho-beclin-1 S93 (clone D9A5G)	Cell Signaling Technology	Cat#14717; RRID: AB_2688032
Rabbit polyclonal anti-phospho-ULK1 S757	Cell Signaling Technology	Cat#6888
Rabbit monoclonal anti-phospho-ULK1 S317 (clone D2B6Y)	Cell Signaling Technology	Cat#12753; RRID: AB_2687883
Rabbit monoclonal anti-ACC (clone C83B10)	Cell Signaling Technology	Cat#3676; RRID: AB_2219397
Rabbit monoclonal anti-phospho-ACC S79 (clone D7D11)	Cell Signaling Technology	Cat#11818; RRID: AB_2687505
Rabbit monoclonal anti-Raptor (clone 24C12)	Cell Signaling Technology	Cat#2280; RRID: AB_561245
Rabbit polyclonal anti-phospho-Raptor S792	Cell Signaling Technology	Cat#2083; RRID: AB_2249475
Rabbit monoclonal anti-mTOR (clone 7C10)	Cell Signaling Technology	Cat#2983; RRID: AB_2105622
Mouse monoclonal anti-S6 (clone 54D2)	Cell Signaling Technology	Cat#2317; RRID: AB_2238583
Rabbit monoclonal anti-phospho-S6 S235/236 (clone D57.2.2E)	Cell Signaling Technology	Cat#4858; RRID: AB_916156
Rabbit monoclonal anti-phospho-S6K T389 (clone 108D2)	Cell Signaling Technology	Cat#9234; RRID: AB_2269803
Rabbit monoclonal anti-phospho-p38 T180/182 (clone D3F9)	Cell Signaling Technology	Cat#4511; RRID: AB_2139682
Rabbit monoclonal anti-phospho-NF-κB S536 (clone 93H1)	Cell Signaling Technology	Cat#3033; RRID: AB_331284
Rabbit polyclonal anti-LC3B	MBL	Cat#PM036; RRID: AB_2274121
Mouse monoclonal anti-Vinculin (clone hVIN-1)	Sigma-Aldrich	Cat#V9131; RRID: AB_477629
Mouse monoclonal anti-beta-Actin (clone AC-15)	Sigma-Aldrich	Cat#A5441; RRID: AB_476744
Rabbit polyclonal anti-LC3B	Novus Biologicals	Cat#NB100-2220; RRID: AB_1109175
Rat monoclonal anti-DYKDDDDK Epitope Tag (clone l5)	Novus Biologicals	Cat#NBP1-06712; RRID: AB_1625981)
Mouse monoclonal anti-LPS of *Salmonella* FITC (clone 1E6)	Santa Cruz Biotechnology	Cat#SC-52223; RRID: AB_630226
Mouse monoclonal anti-VPS34 (clone F-11)	Santa Cruz Biotechnology	Cat#SC-365404; RRID: AB_10846189
Mouse monoclonal anti-GST (clone B-14)	Santa Cruz Biotechnology	Cat#SC-138; RRID: AB_627677
Rabbit monoclonal anti-p62 (clone EPR18351)	Abcam	Cat#ab207305
Rabbit monoclonal anti-S6K (clone E343)	Abcam	Cat#ab32529; RRID: AB_777800
Rabbit polyclonal anti-ATG14	Abcam	Cat#ab139727
Rabbit monoclonal anti-ULK1 555 (clone EPR4885(2))	Abcam	Cat#ab206612
Rat monoclonal anti-LAMP1 (clone 1D4B)	Abcam	Cat#ab25245; RRID: AB_449893
Guinea pig polyclonal anti-p62	Progen Biotechnik	Cat#GP62-C; RRID: AB_2687531

(*Continued on next page*)

Continued

REAGENT or RESOURCE	SOURCE	IDENTIFIER
Rabbit polyclonal anti-Sirtuin-1	Upstate/Millipore	Cat#07-131
Bacterial and Virus Strains		
Wild-type *Salmonella* Typhimurium strain SL1344	Dr. Sad, University of Ottawa	Sad et al., 2008; RRID: WB-STRAIN:SL1344
InvA mutant *Salmonella* Typhimurium and SsaR mutant *Salmonella* Typhimurium	Dr. Sad, University of Ottawa	Sad et al., 2008
Wild-type *Shigella flexneri* 5a strain M90T-Sm	Dr. Campbell-Valois, University of Ottawa	Campbell-Valois et al., 2015
Wild-type adherent-invasive *E. coli* (AIEC) strain NRG857c	Dr. Coombes, McMaster University	Small et al., 2013
DH5α Competent Cells	ThermoFisher Scientific	Cat#18265017
Murine norovirus 1	Dr. Thomas Smith, University of Texas	Katpally et al., 2008
Chemicals, Peptides, and Recombinant Proteins		
LPSs from *Escherichia coli* 0111:B4	Sigma-Aldrich	Cat#L4391-1MG
Resiquimod	Sigma-Aldrich	Cat#SML0196-10MG
Filipin III from Streptomyces filipinensis	Sigma-Aldrich	Cat#F4767-1MG
Torin-1	Sigma-Aldrich	Cat#475991-10MG
Chloroquine	Sigma-Aldrich	Cat#C6628-25G
Sodium salicylate	Sigma-Aldrich	Cat#S3007-500G
DAPI for nucleic acid staining	Sigma-Aldrich	Cat#D9542-1MG
Streptomycin sulfate salt	Sigma-Aldrich	Cat#S6501-25G
Proteinase K	New England BioLabs	Cat#P8107S
Neuron-derived exosomes	Dr. Gibbings, University of Ottawa	N/A
Digitonin	VWR	Cat#10188-874
Iron Supplemented Bovine Calf Serum LOT#141A15	VWR	Cat#10158-358
Bafilomycin A1	VWR	Cat#89156-932
Gentamicin	ThermoFisher Scientific	Cat#15750060
Fetal Bovine Serum	ThermoFisher Scientific	Cat#12483020
Puromycin	ThermoFisher Scientific	Cat#A1113803
Carbenicillin	ThermoFisher Scientific	Cat#BP26485
Adenosine 5′-triphosphate disodium salt hydrate	ThermoFisher Scientific	Cat#BP41325
Trypan blue	Bio-Rad	Cat#1450102
Compound C	Tocris	Cat#309310
Dynasore	Abcam	Cat#ab120192
Protein A Affinity Resin	Repligen	Cat#CA-PRI-0100
L-α-PtdIns	Avanti polar lipids	Cat#840042P
Protease inhibitor cocktail	Apex BIO	Cat#K1007
Serine/Threonine phosphatase inhibitor cocktail	Apex BIO	Cat#K1012
Critical Commercial Assays		
EZ-10 Spin Column Plasmid DNA Minipreps Kit	BioBasics	Cat#BS614
Invitrogen PureLink Genomic DNA Mini Kit	ThermoFisher Scientific	Cat#K182001
Experimental Models: Cell Lines		
HEK293A	ATCC	CRL-1573
A549	ATCC	CCL-185
MCF-7	ATCC	HTB-22

(*Continued on next page*)

Continued

REAGENT or RESOURCE	SOURCE	IDENTIFIER
LKB1 knockout MEF	Russell Jones	N/A
Wild-type and AMPK knockout MEF	Russell Jones	N/A
Wild-type HCT116	ATCC	CCL-247
NOD1 knockout, NOD2 knockout, and NOD1/2 knockout HCT116	Dr. Girardin, University of Toronto	Gaudet et al., 2017
IRAK knockout HCT116	This paper	N/A
TRAF6 knockout HCT116	This paper	N/A
STING knockout HCT116	This paper	N/A
Bone marrow deprived macrophages (BMDMs)	Dr. Fullerton, University of Ottawa	Galic et al., 2011
Oligonucleotides		
IRAK guide RNA sequences: CACCGTC TTGTACGAGGTGCCGCCC and CACC GCCGACTGGTGCCAGTTCGGT	ThermoFisher Scientific	N/A
TRAF6 guide RNA sequence: CACCGT GTTACAGCGCTACAGGAGC	ThermoFisher Scientific	N/A
STING guide RNA sequences: CACCG AGAGCACACTCTCCGGTACC and CACCGCTGGGACTGCTGTTAAACG	ThermoFisher Scientific	N/A
Recombinant DNA		
Plasmid: pcdna3 flag - ULK1 WT	Addgene	27636

CONTACT FOR REAGENT AND RESOURCE SHARING

Further information and requests for resources and reagents should be directed to and will be fulfilled by the Lead Contact, Ryan Russell (ryan.russell@mailuottawa.ca).

EXPERIMENTAL MODEL AND SUBJECT DETAILS

Cell Culture

MEF, HEK293A, and HCT116 were cultured in DMEM supplemented with 10% Bovine Calf Serum (BCS, VWR). A549 cells were cultured in F-12K medium supplemented with 10% Fetal Bovine Serum (FBS, Hyclone). MCF-7 were cultured in EMEM supplemented with 10% FBS. Amino acid free medium was made according to GIBCO standard recipe omitting all amino acids and supplemented as above without addition of non-essential amino acids and substitution with dialyzed FBS. Media was changed 1 hour before experiments. Bone marrow deprived macrophages (BMDMs) were a kind gift from Dr. Fullerton, University of Ottawa. LKB1 wild-type and knock-out MEF cells were a generous gift from Russell Jones. NOD1 knock-out, NOD2 knock-out, and NOD1/2 knock-out HCT116 cells were previously characterized(Gaudet et al., 2017) and a kind gift from Dr. Girardin, University of Toronto.

Generation of Stable Cell Line

Flag ULK1 (Addgene, 27636) with puromycin resistance was used to create a stable polyclonal population of cells expressing near endogenous level of ULK1. The cells expressing tagged ULK1 were maintained by 1 μg/mL of puromycin.

Generation of knock-out cell lines using CRISPR/Cas9

HCT116 IRAK, TRAF6, and STING knockouts were generated using CRISPR/Cas9 targeting exon 1. IRAK guide RNA sequences: CACCGTCTTGTACGAGGTGCCGCCC and CACCGCCGACTGGTGCCAGTTCGGT. TRAF6 guide RNA sequence: CACCGTGTTACAGCGCTACAGGAGC. STING guide RNA sequences: CACCGAGAGCACACTCTCCGGTACC and CACCGC TGGGACTGCTGTTAAACG.

METHOD DETAILS

Bacterial Infection

Wild-type (SL1344), Inva mutant, and SsaR mutant *Salmonella* were generated as described previously(Sad et al., 2008). Wild-type *Shigella* was obtained from Dr. Campbell-Valois, University of Ottawa. AIEC was a generous gift from Dr. Coombes, McMaster

University. Bacteria were grown in Luria-Bertani broth. Murine norovirus (MNV) were generous gifts from Dr. Thomas Smith, University of Texas. DH5α Competent Cells (Cat#18265017) were purchased from ThermoFisher Scientific. Overnight bacterial cultures of *Salmonella* were diluted 30-fold and grown to log phase (OD_{600} = 1.5), collected by centrifugation 10,000 g for 2 min, and resuspended in 1 mL of PBS. Bacterial stock was then diluted 10-fold (MOI = 450) in DMEM supplemented with heat-inactivated BCS for infection. Cells cultured in antibiotic-free medium were infected with *Salmonella* and incubated at 37°C in 5% CO_2 for the indicated time. Cells were washed in PBS once before lysis. For gentamycin assays, the cells were infected, preceded or followed by incubation with gentamicin (50 μg/mL, ThermoFisher Scientific) for 0.5 hour. Gentamicin was added before and after bacterial infection to control for potential off-target effects of the drug (for example: the possibility that mTORC1 signaling may be altered by gentamycin addition). Bacteria were killed by incubation with 4% paraformaldehyde (PFA) for 15 min.

Preparation of bacterial supernatant

Overnight bacterial cultures of *Salmonella* were diluted 30-fold and grown to log phase (OD_{600} = 1.5), 1ml was collected by centrifugation at 10,000 g for 2 min and resuspended in 5 mL of heat-inactivated DMEM. *Salmonella*-containing media was then shaken at 250 rpm for the indicate time points. Following the incubation, the bacteria were removed by centrifugation (10000 g for 2 min) and supernatant was filtered through a 0.45 uM filter.

OMV Purification

Wild-type *Salmonella* was grown in 4 mL of LB broth supplemented with carbenicillin (ThermoFisher Scientific) at 37°C at 250 rpm. After 16-18 hours of incubation, all of bacteria were transferred to 1.5 L of LB and were shaken for extra 18 hours. The bacteria were then removed by centrifugation (15000 rpm, 30 min, 4°C). The collected supernatant was vacuum filtered and incubated overnight with OMV precipitation solution (300 g of PEG, 43.9g NaCl in water up to 1L, 3x stock) at 4°C. OMVs were harvested by two centrifugations (4200 rpm, 30 min, 4°C) and one ultracentrifugation (28500 rpm, 3 hours, 4°C). The pellets were suspended in clear DMEM and stored at 4°C for future use. The size of OMV was determined by Nanoparticle Tracking Analysis using a Particle Metrix Zetasizer (Particle Metrix GmbH, Meerbusch, Germany). OMV samples diluted 1:100000 in PBS were captured with 11 positions. Data were analyzed with the built-in ZetaView 8.02.31 software. The concentration of OMV stock is $3.6*10^{11}$ particles/mL.

OMV modifications

Heat shock

Heat-inactivated OMVs were warmed at 55°C for 5 minutes and diluted in complete media prior to treatment.

Paraformaldehyde Fixation

OMVs were fixed with 4% PFA for 20 min followed by inactivation with 1M Tris pH-8 for 30 min. Fixed OMVs were ultracentrifuged at 100 000 g for 30 min, washed 2x with 1M Tris pH = 8, and re-suspended in complete media prior to treatment.

Proteinase Treatment

OMVs were incubated in the presence or absence of proteinase K (1.6 units), or buffer alone for 30 mins prior to nucleofection (Lonza, used X-001 setting). The nucleofected OMVs were resuspended, washed 3x with PBS, and harvested by ultracentrifugation (100 000 g for 30 min).

Western blot and Immunoprecipitation

Whole cell lysates were generated by direct lysis with 1X denaturing SDS sample buffer. Samples were boiled for 10 min at 95°C and resolved by SDS-PAGE. Immune complexes were obtained from cells lysed in mild lysis buffer [10mM Tris pH 7.5, 10 mM EDTA, 100 mM NaCl, 50 mM NaF, 1% NP-40, supplemented at time of lysis with protease and phosphatase inhibitor cocktails –EDTA (APExBIO)]. Protein A beads (Repligen) were washed 1X with MLB and mixed with antibodies and cleared cell lysates for 1.5-3 hours followed by one wash with MLB and inhibitors and 4 washes with MLB alone. Beads were boiled in 1X denaturing sample buffer for 10 min before resolving by SDS-PAGE.

Immunofluorescence

Cells were plated on IBDI-treated coverslips the night before treatments. Cells were fixed by 4% PFA in PBS for 15 min, followed by permeabilization with 50 μg/mL digitonin (VWR) in PBS for 10 min. Cells were blocked in blocking buffer (1% BSA and 2% serum in PBS) for 30 min then incubated with primary antibodies in the same buffer for one hour at room temperature. Slides were washed 2X in PBS and 1X in blocking buffer followed by incubation of secondary antibodies in blocking buffer for one hour at room temperature. Slides were washed 3X in PBS, stained with DAPI (Sigma-Aldrich), and mounted. Images were captured with inverted epifluorescent Zeiss AxioObserver.Z1. In the case of outside/inside bacterial staining, before permeabilization, the cells were incubated with primary and following secondary antibodies in blocking buffer, accompanied by 3X PBS washes in between.

In vitro ULK1 Kinase Assay

ULK1 proteins were immunoprecipitated and extensively washed with MLB (once) and RIPA buffer (50 mM Tris at pH 7.5, 150 mM NaCl, 50 mM NaF, 1 mM EDTA, 1 mM EGTA, 1% SDS, 1% Triton X-100 and 0.5% deoxycholate) once, followed by washing with MLB buffer once followed by equilibration with ULK1 assay buffer (kinase base buffer supplemented with 0.05 mM DTT and 10 μM cold

ATP (ThermoFisher Scientific) per reaction). Reactions were rocked at 250 rpm at 37°C for 30 min and quenched by direct addition of 4X sample buffer followed by 10 min boiling and resolution by SDS-PAGE. The analysis of kinase reactions necessitated the separation of the kinase and substrate. *In vitro* kinase reactions were analyzed by western blot with the phospho-Beclin-1 antibody.

In vitro VPS34 Lipid Kinase Assay

Immunoprecipitated proteins were incubated with 40 μL of 1X kinase base buffer (200 mM HEPES pH 7.4, 50 mM $MgCl_2$, 10 mM EGTA, and 4 mM EDTA) supplemented with 0.5 mg/mL PtdIn (Avanti polar lipids), 0.25 mM cold ATP, 25 mM $MnCl_2$, and 0.25 mM DTT at 37°C for 30 min with vigorous shaking. After the reaction, the supernatant was separated from the beads and analyzed by dot blot. Beads were boiled in 1X denaturing sample buffer for 10 min before resolving by SDS-PAGE for the inputs.

Colony Forming Unit (CFU) Assay

Cells were infected with *Salmonella* for 1 hour. The infected cells were washed 2X and incubated with media containing 100 μg/mL Gentamicin for 0.5 hour, followed by 4-hour incubation with media containing 50 μg/mL Gentamicin. The samples were rinsed 3X with PBS and lysed with CFU buffer (0.1% Triton X-100 and 0.01% SDS in PBS). The lysates were serially diluted and plated onto LB agar plates containing Streptomycin (Sigma-Aldrich). The plates were incubated at 37°C for 16-18 hours and the colonies were counted to determine the number of CFU.

QUANTIFICATION AND STATISTICAL ANALYSIS

Quantification of Immunofluorescence

Epifluorescent microscopy images were used to determine colocalization using an automated protocol built in the Volocity PerkinElmer imaging software to reduce bias. The same protocol was applied to each field of view and across samples. Quantification was performed on representative experiments with an average of 27 unique fields of view.

Statistical Analysis

Statistical analysis was performed on at least two biological repeats. Error bars represent the standard deviation in normalized fold changes in observed induction or repression. Statistical significance was determined using paired Student's one-tailed t test for at least two datasets. All statistical parameters for assays in this study are shown in the corresponding figure legends.